



UNIVERSITÀ
DEGLI STUDI
DI BRESCIA

unibs.it



ASSOCIAZIONE SCIENTIFICA
"GIULIO DE MARCHI"

Giornata di studio in memoria di Baldassare Bacchi

Brescia, 18 November 2019

Advances in stochastics of hydroclimatic extremes

Bonus: How to Avoid Two Steps Back



Demetris Koutsoyiannis

School of Civil Engineering, National Technical University of Athens, Greece
(dk@itia.ntua.gr, <http://www.itia.ntua.gr/dk/>)

Visiting professor, Dipartimento Ingegneria Civile, Chimica, Ambientale e dei Materiali (DICAM), Università di Bologna

Presentation available online: <http://www.itia.ntua.gr/2010/>

Baldo Bacchi: a multidimensional noble man, a frank guy, a great humourist, a rigorous scientist



Baldassare Bacchi
- PO di Costruzioni
Idrauliche e
Marittime e
Idrologia (SSD
ICAR/02)



Baldo Bacchi's research team in 2015 with faculty members, doctoral students and post-docs; from left to right: Eleni Michailidi, Marco Pilotti (PA SSD ICAR/01), Luca Milanesi, Stefano Barontini (RC SSD ICAR/02), Giulia Valerio, Baldo Bacchi, Roberto Ranzi (PO SSD ICAR/02), Matteo Balistrocchi, Massimo Tomirotti, Alessandra Viani.

Baldo Bacchi's seminal contributions to the stochastics of hydrological extremes

WATER RESOURCES RESEARCH, VOL. 28, NO. 10, PAGES 2773-2782, OCTOBER 1992

Analysis of the Relationships Between Flood Peaks and Flood Volumes Based on Crossing Properties of River Flow Processes

BALDASSARE BACCHI

Dipartimento di Ingegneria Civile, Università di Brescia, Brescia, Italy

ARMANDO BRATH

Dipartimento di Ingegneria e Fisica dell'Ambiente, Università della Basilicata, Potenza, Italy

NATH T. KOTTEGODA

Dipartimento di Ingegneria Idraulica, Politecnico di Milano, Milan, Italy



Journal of Hydrology 155 (1994) 225-236

Journal
of
Hydrology

[4]

Bivariate exponential model applied to intensities and durations of extreme rainfall

Baldassare Bacchi^{*-a}, Gianfranco Becciu^a, Nath.T. Kottegoda^b

^a*Dipartimento di Ingegneria Civile, Università di Brescia, Via Valotti 9, 25100 Brescia, Italy*

^b*Dipartimento di Ingegneria Idraulica, Ambientale e del Rilevamento, Politecnico di Milano, Piazza Leonardo da Vinci 32, 20133 Milano, Italy*

(Received 1 August 1991; revision accepted 20 July 1993)



ELSEVIER

Atmospheric Research 42 (1996) 123-135

ATMOSPHERIC
RESEARCH

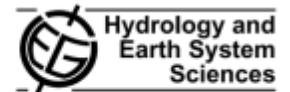
On the derivation of the areal reduction factor of storms

Baldassare Bacchi, Roberto Ranzi *

Department of Civil Engineering, University of Brescia, Via Branze 38, I-25123 Brescia, Italy

Received 4 December 1994; accepted 25 May 1995

Hydrol. Earth Syst. Sci., 15, 1959-1977, 2011
www.hydrol-earth-syst-sci.net/15/1959/2011/
doi:10.5194/hess-15-1959-2011
© Author(s) 2011. CC Attribution 3.0 License.



Modelling the statistical dependence of rainfall event variables through copula functions

M. Balistocchi and B. Bacchi

Hydraulic Engineering Research Group, Department of Civil Engineering Architecture Land and Environment DICATA, University of Brescia, 25123 Brescia, Italy

The general framework: Seeking theoretical consistency in analysis of geophysical data (Using *stochastics*)

Project

Seeking Theoretical Consistency in Analysis of Geophysical Data (Using Stochastics)

Demetris Koutsoyiannis · Panayiotis Dimitriadis · Theano (Any) Iliopoulou · [Show all 6 collaborators](#)

Goal: Analysis of geophysical data is (explicitly or implicitly) based on stochastics, i.e. the mathematics of random variables and stochastic processes. These are abstract mathematical objects, whose properties...

[Show details](#)

Fully NOT Funded (NOT even by Big Oil)

Book in preparation:

D. Koutsoyiannis, *Stochastics of Hydroclimatic Extremes – A Cool Look at Risk* (2020)

Is “stationarity dead” and is there “rainfall intensification”?

POLICYFORUM

CLIMATE CHANGE

Stationarity Is Dead: Whither Water Management?

P. C. D. Milly,^{1*} Julio Betancourt,² Malin Falkenmark,³ Robert M. Hirsch,⁴ Zbignij Kundzewicz,⁵ Dennis P. Lettenmaier,⁶ Ronald J. Stouffer⁷

LETTERS

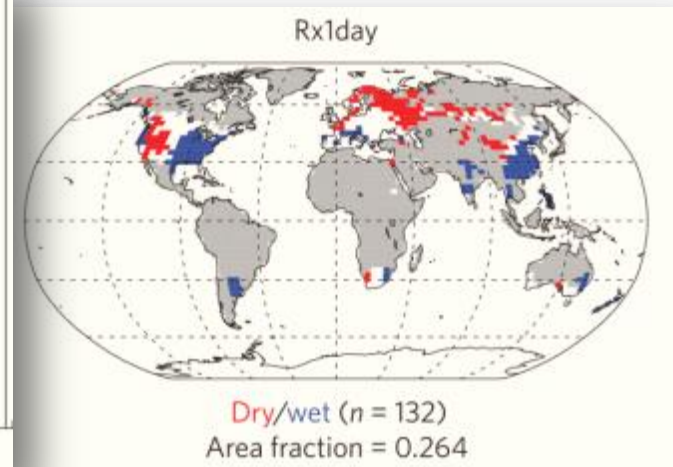
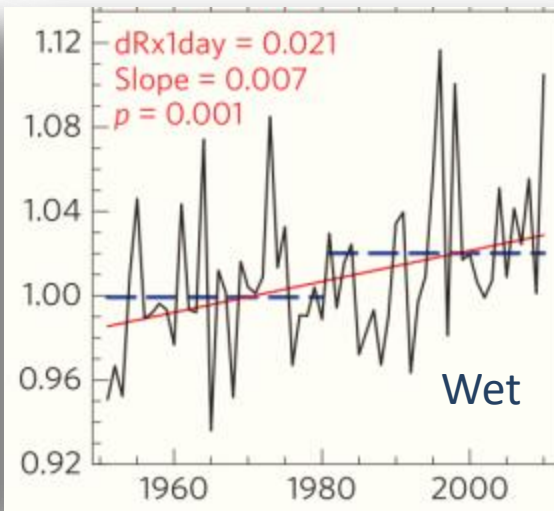
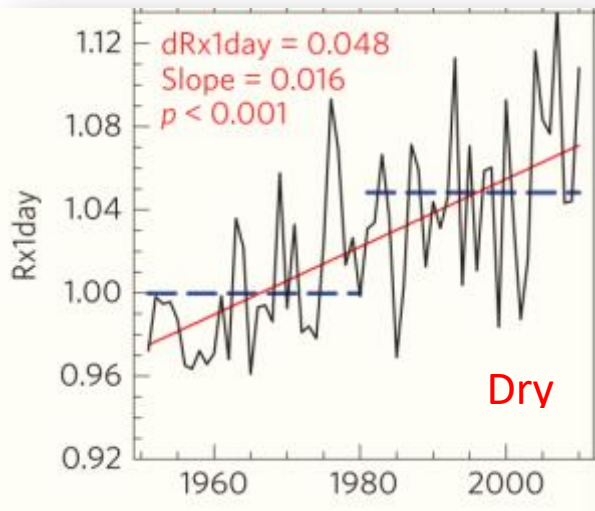
PUBLISHED ONLINE: 7 MARCH 2016 | DOI: 10.1038/NCLIMATE2941

nature
climate change

More extreme precipitation in the world's dry and wet regions

Markus G. Donat^{1*}, Andrew L. Lowry¹, Lisa V. Alexander¹, Paul A. O’Gorman² and Nicola Maher¹

The climatic value of annual maximum daily rainfall of the 30-year period 1980 – 2010, compared to that of 1960-80, is greater by **5%** for dry areas and by **2%** for wet areas (Donat et al., 2016).



Climate change impacts on the scientific level of hydrology: The surge of studies of nonstationary extremes

AGU PUBLICATIONS

Water Resources Research

RESEARCH ARTICLE Predicting nonstationary flood frequencies: Evidence supports an updated stationarity thesis in the United States
10.1002/2016WR019676

atmosphere

Article
An Uncertainty Investigation of RCM Downscaling Ratios in Nonstationary Extreme Rainfall IDF Curves

Journal of Hydrology 519 (2014) 2040–2048



Contents lists available at ScienceDirect

Journal

journal homepage: www

Nat. Hazards Earth Syst. Sci. Discuss., <https://doi.org/10.5194/nhess-2018-290>
Manuscript under review for journal Nat. Hazards Earth Syst. Sci.
Discussion started: 16 October 2018
© Author(s) 2018. CC BY 4.0 License.

Natural Hazards and Earth System Sciences Discussions EGU

Projected intensification of sub-daily and daily rainfall extremes in convection-permitting climate model simulations over North America: Implications for future Intensity-Duration-Frequency curves

in Water Resources 118 (2018) 83–94

is lists available at ScienceDirect

es in Water Resources

ge: www.elsevier.com/locate/advwatres

ng for nonstationary hydrology

OPEN Nonstationary Precipitation Intensity-Duration-Frequency Curves for Infrastructure Design in a Changing Climate

SUBJECT AREAS
CLIMATE SCIENCES
HYDROLOGY

Received
19 June 2014

HYDROLOGICAL SCIENCES JOURNAL, 2018
VOL. 63, NO. 3, 325–352
<https://doi.org/10.1080/02626667.2018.1426858>

Techniques for assessing water infrastructure for nonstationary extreme events: a review

ERDC/CHL CHETN-X-2
March 2016



US Army Corps of Engineers®

Bayesian Inference of Nonstationary Precipitation Intensity-Duration-Frequency Curves for Infrastructure Design

Water Resour Manage (2015) 29:5533–5550
DOI 10.1007/s11269-015-1133-5



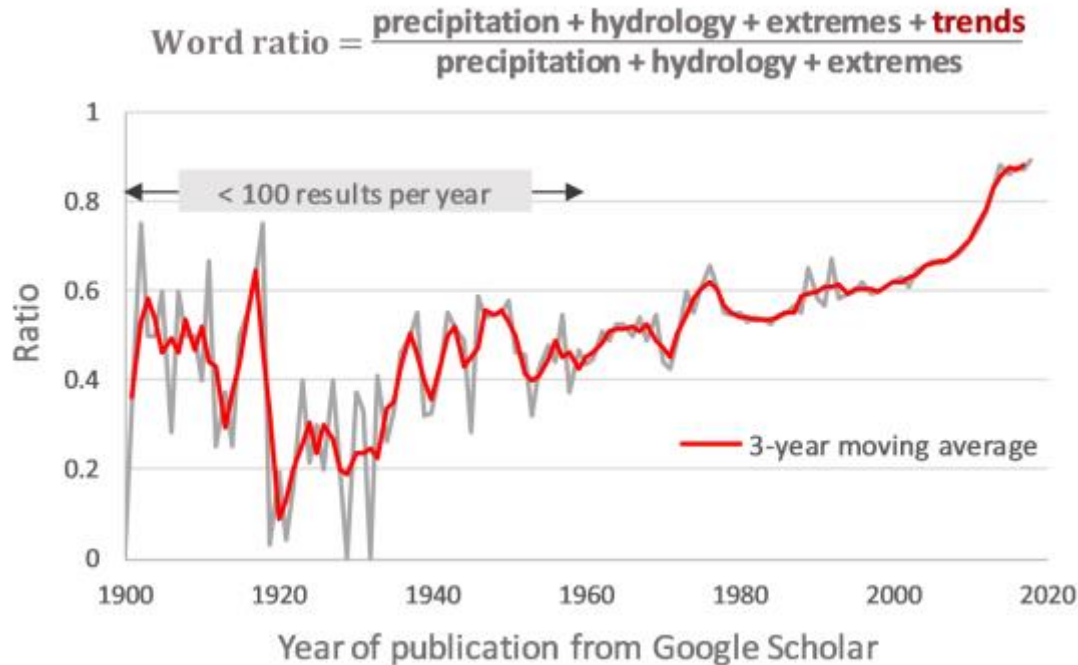
Nonstationary Flood Frequency Analysis for Annual Flood Peak Series, Adopting Climate Indices and Check Dam Index as Covariates



Taylor & Francis
Taylor & Francis Group

Check for updates

Quantification of “steps back” using bibliometrics



In 2018, among the scientific articles, registered by Google Scholar that contained the terms “precipitation”, “hydrology” and “extremes”, 89% also contained the word “trends”.

Since 1920, there has been a rising trend in the frequency of the word “trends”

Since ~2010 there has been an upward shift in that frequency.

Source: Iliopoulou and Koutsoyiannis (2019)

Note: It appears that Baldo Bacchi had not been severely affected by climate change...

None of his articles contained the terms “trend”, “trends”, “nonstationary”, “nonstationarity” in its title.

author:b-bacchi intitle:trends OR intitle:trend OR intitle:nonstationary OR intitle:nonstationarity

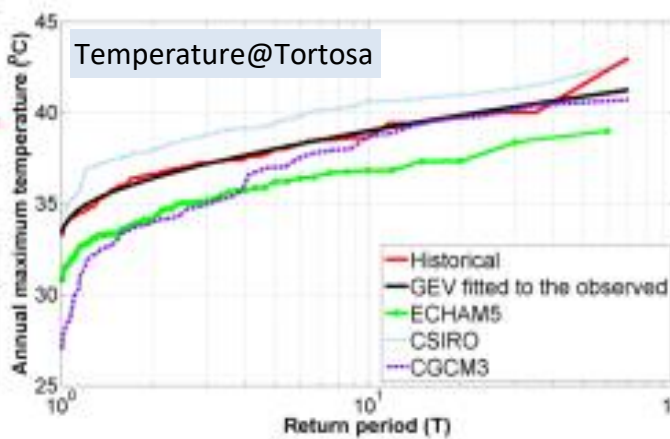
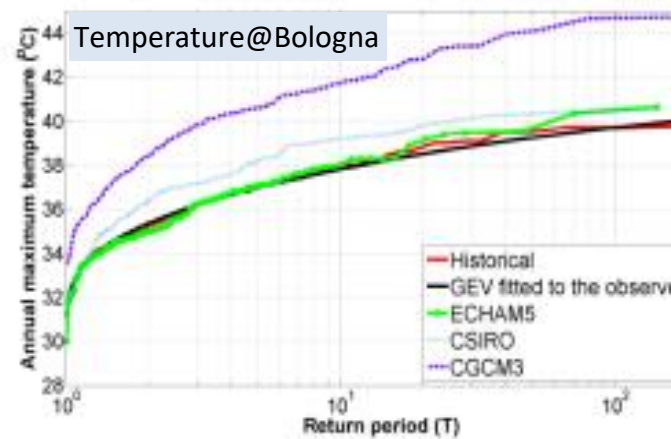
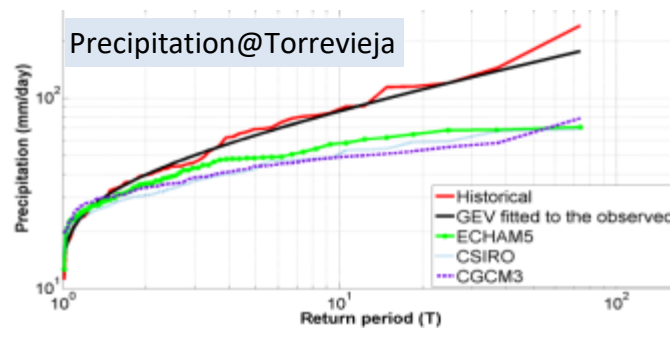
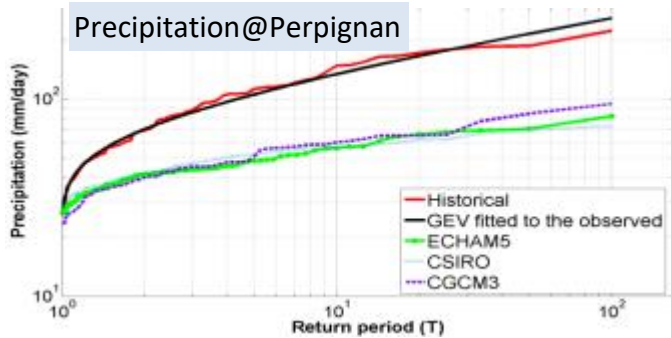
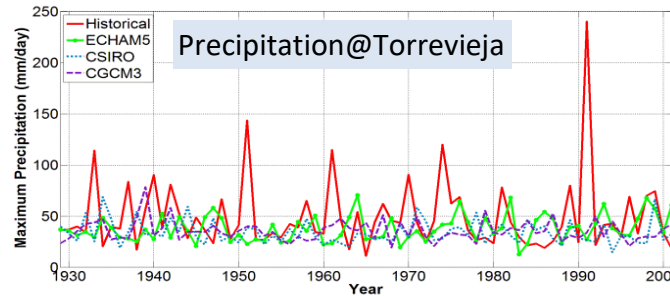
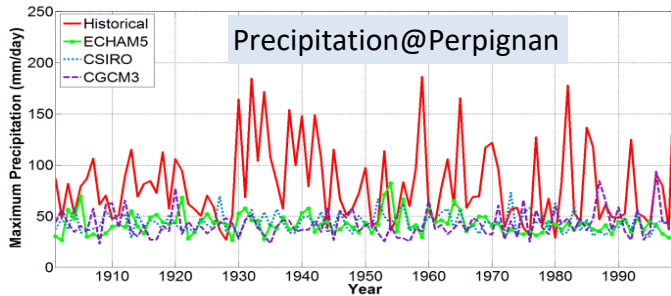
Scholar

Your search - author:b-bacchi intitle:trends OR intitle:trend OR intitle:nonstationary OR intitle:nonstationarity - did not match any articles.

Suggestions:

- Make sure all words are spelled correctly.
- Try different keywords.
- Try more general keywords.
- Try your query on the entire web

Do climate models allow a nonstationary approach on extremes?



Tsaknias et al. (2016—**multirejected paper**) tested the reproduction of extreme events by three climate models of the IPCC AR4 at 8 test sites in the Mediterranean with long time series of temperature and precipitation.

They concluded that climate models are not able even to approach the natural behaviour in extreme events.

The graphs show plots of time series and probability distributions of annual maximum daily precipitation and temperature in comparison with climate model results.

Both stationarity and ergodicity are abstract mathematical concepts; hence they are immortal!

AGU PUBLICATIONS

Water Resources Research

COMMENTARY

10.1002/2014WR016092

Modeling and mitigating natural hazards: Stationarity is immortal!

Alberto Montanari¹ and Demetris Koutsoyiannis²

¹Department of Civil, Chemical, Environmental, and Materials Engineering, University of Bologna, Bologna, Italy,

²Department of Water Resources and Environmental Engineering, School of Civil Engineering, National Technical University of Athens, Athens, Greece

Correspondence to:

A. Montanari,
alberto.montanari@unibo.it

Citation:

Montanari, A., and D. Koutsoyiannis (2014), Modeling and mitigating natural hazards: Stationarity is immortal, *Water Resour. Res.*, 50, doi:10.1002/2014WR016092

Abstract Environmental change is a reason of relevant concern as it is occurring at an unprecedented pace and might increase natural hazards. Moreover, it is deemed to imply a reduced representativity of past experience and data on extreme hydroclimatic events. The latter concern has been epitomized by the statement that "stationarity is dead." Setting up policies for mitigating natural hazards, including those triggered

1174

Hydrological Sciences Journal – Journal des Sciences Hydrologiques, 60 (7–8) 2015

<http://dx.doi.org/10.1080/02626667.2014.959959>

Special issue: *Modelling Temporally-variable Catchments*

Negligent killing of scientific concepts: the stationarity case

Demetris Koutsoyiannis¹ and Alberto Montanari²

Stationarity and ergodicity are tightly connected to each other.

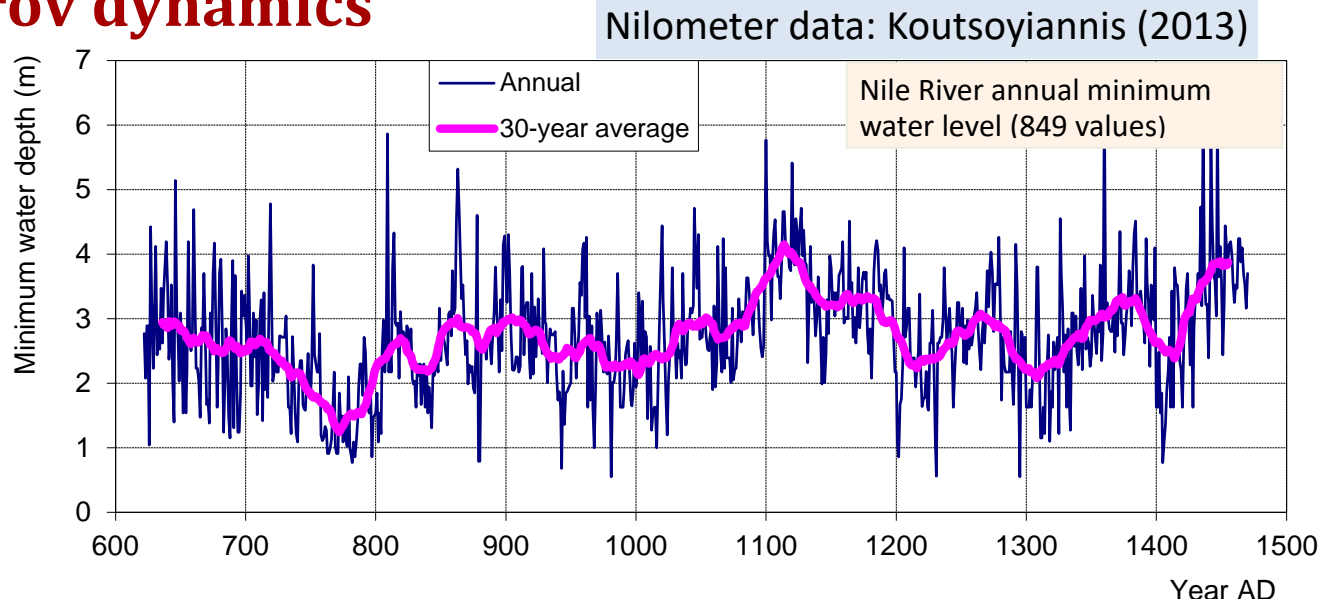
Without stationarity there cannot be ergodicity.

Without ergodicity inference from data would not be possible.

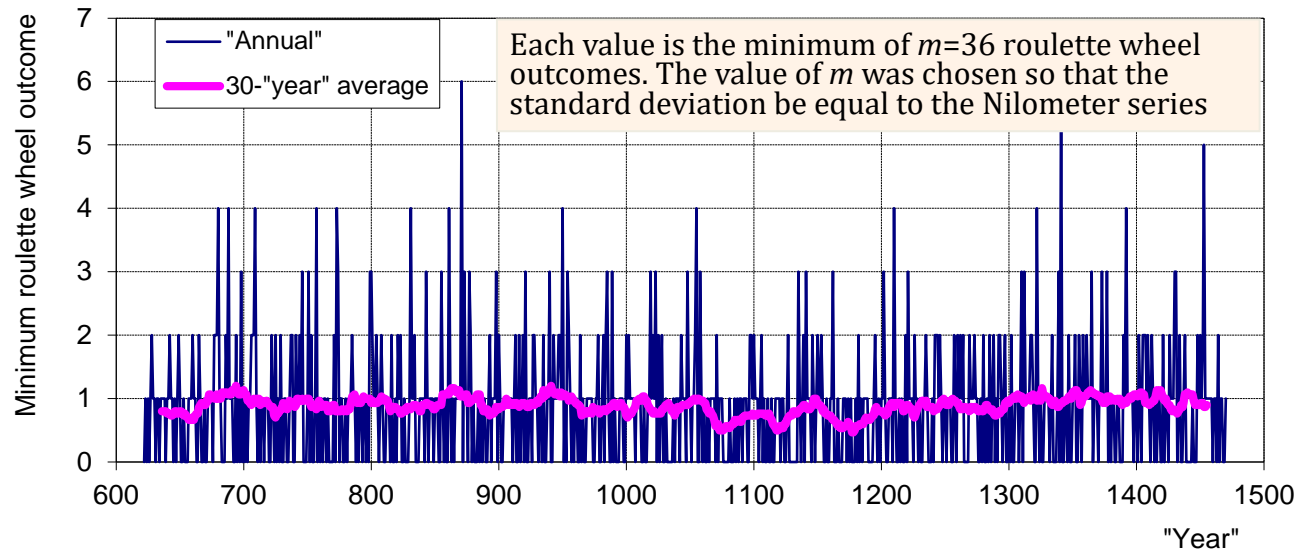
Ironically, several studies use time series data to estimate statistical properties, as if the process were ergodic, while at the same time what they (cursorily) estimate may falsify the ergodicity hypothesis.

Stationary description of Earth's perpetual change: Hurst-Kolmogorov dynamics

Structured randomness



Pure randomness



The climacogram: A simple statistical tool to quantify change across time scales

- Take the Nilometer time series, x_1, x_2, \dots, x_{849} , and calculate the sample estimate of variance $\gamma(1)$, where the argument (1) indicates time scale (1 year)
- Form a time series at time scale 2 (years):

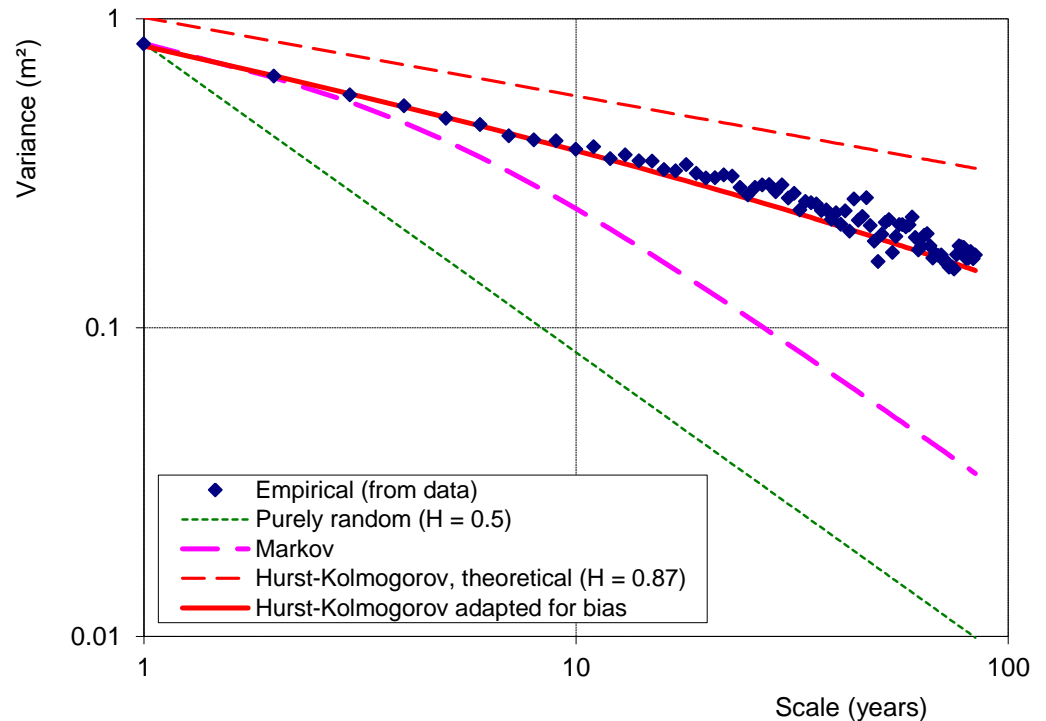
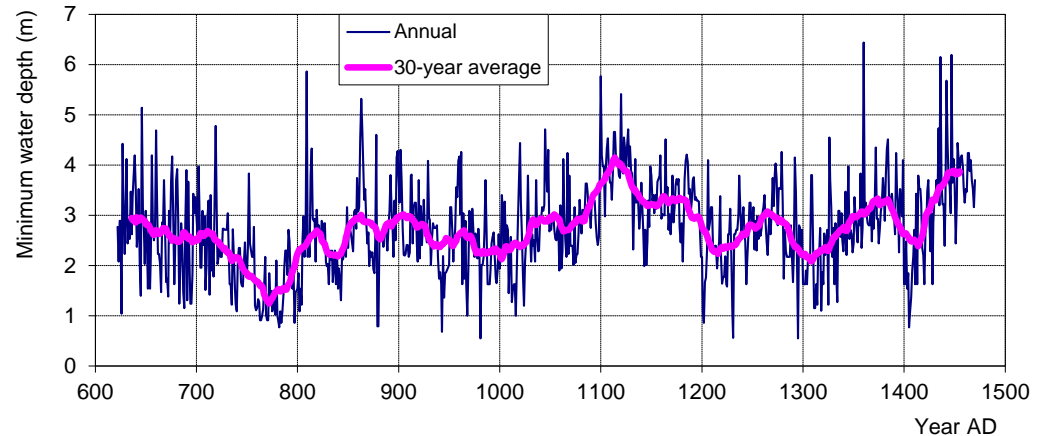
$$x_1^{(2)} := \frac{x_1 + x_2}{2}, x_2^{(2)} := \frac{x_3 + x_4}{2}, \dots, x_{424}^{(2)} := \frac{x_{847} + x_{848}}{2}$$

and calculate the sample estimate of the variance $\gamma(2)$.

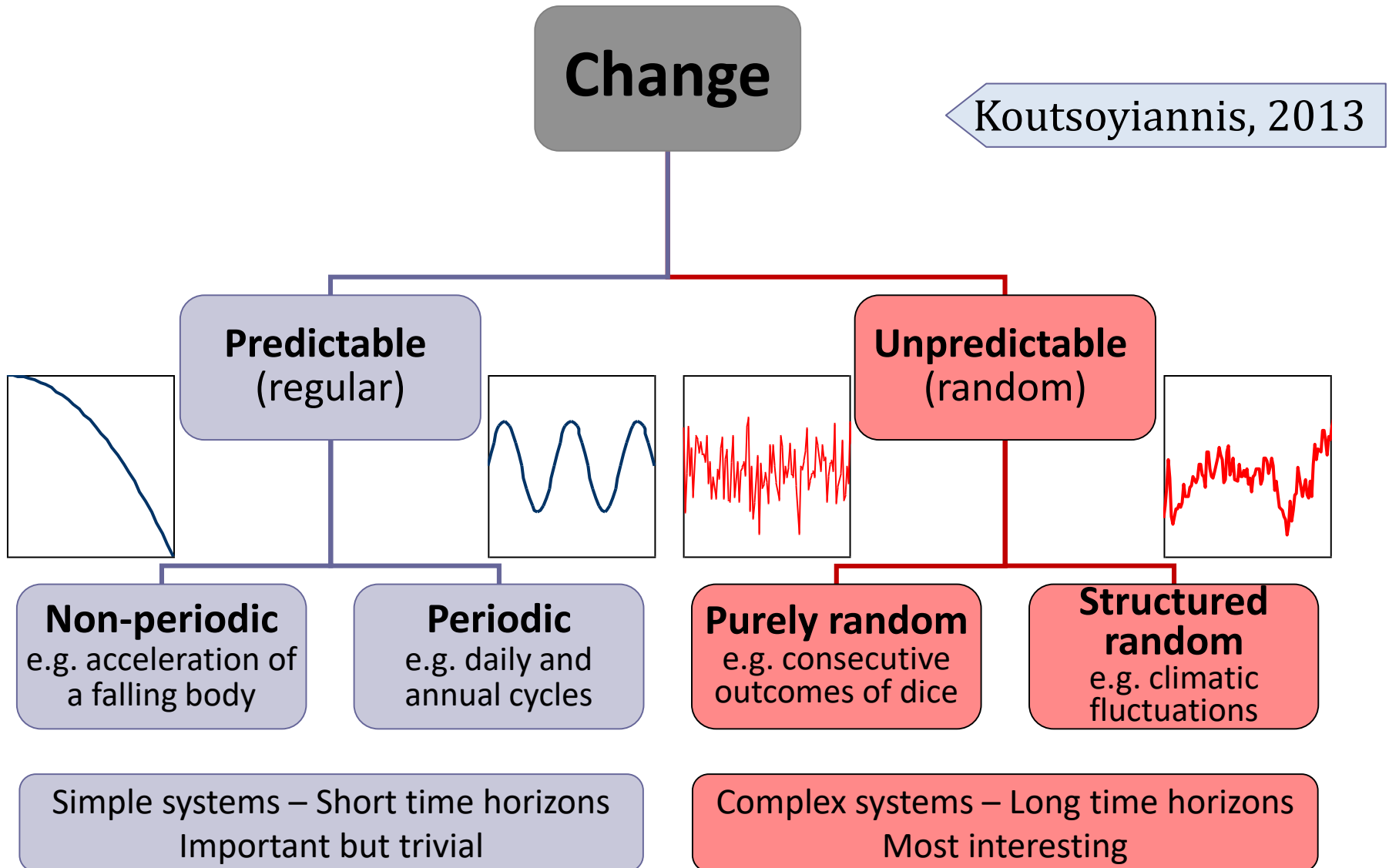
- Repeat the same procedure and form a time series at time scale 3, 4, ... (years), up to scale 84 (1/10 of the record length) and calculate the variances $\gamma(3), \gamma(4), \dots, \gamma(84)$.
- The **climacogram** is the variance $\gamma(\kappa)$ as a function of scale κ ; it is visualized as a double logarithmic plot of $\gamma(\kappa)$ vs. κ .
- If the time series x_τ represented a pure random process, the climacogram would be a straight line with slope -1 (the proof is very easy).
- In real world processes, the slope is different from -1 , designated as $2H - 2$, where H is the so-called Hurst coefficient ($0 < H < 1$).
- The scaling law $\gamma(\kappa) = \gamma(1) / \kappa^{2-2H}$ defines the **Hurst-Kolmogorov (HK) process**.
- High values of H (> 0.5) indicate **enhanced change** at large scales, else known as **long-term persistence**, or strong **clustering** (grouping) of similar values.

The climacogram of the Nilometer time series

- The Hurst-Kolmogorov process seems consistent with reality.
- The Hurst coefficient is $H = 0.87$ (Similar H values are estimated from the simultaneous record of maximum water levels and from the modern, 131-year, flow record of the Nile flows at Aswan).
- The Hurst-Kolmogorov behaviour, seen in the climacogram, indicates that:
 - (a) long-term changes are more frequent and intense than commonly perceived, and
 - (b) future states are much more uncertain and unpredictable on long time horizons than implied by pure randomness.



Change and predictability



Data for illustration 1: Daily precipitation in Bologna

Bologna, Italy (44.50°N, 11.35°E, +53.0 m).

Available from the Global Historical Climatology Network (GHCN) – Daily.

Uninterrupted for the period 1813-2007: 195 years.

For the period 2008-2018, daily data are provided by the repository Dext3r of ARPA Emilia Romagna.

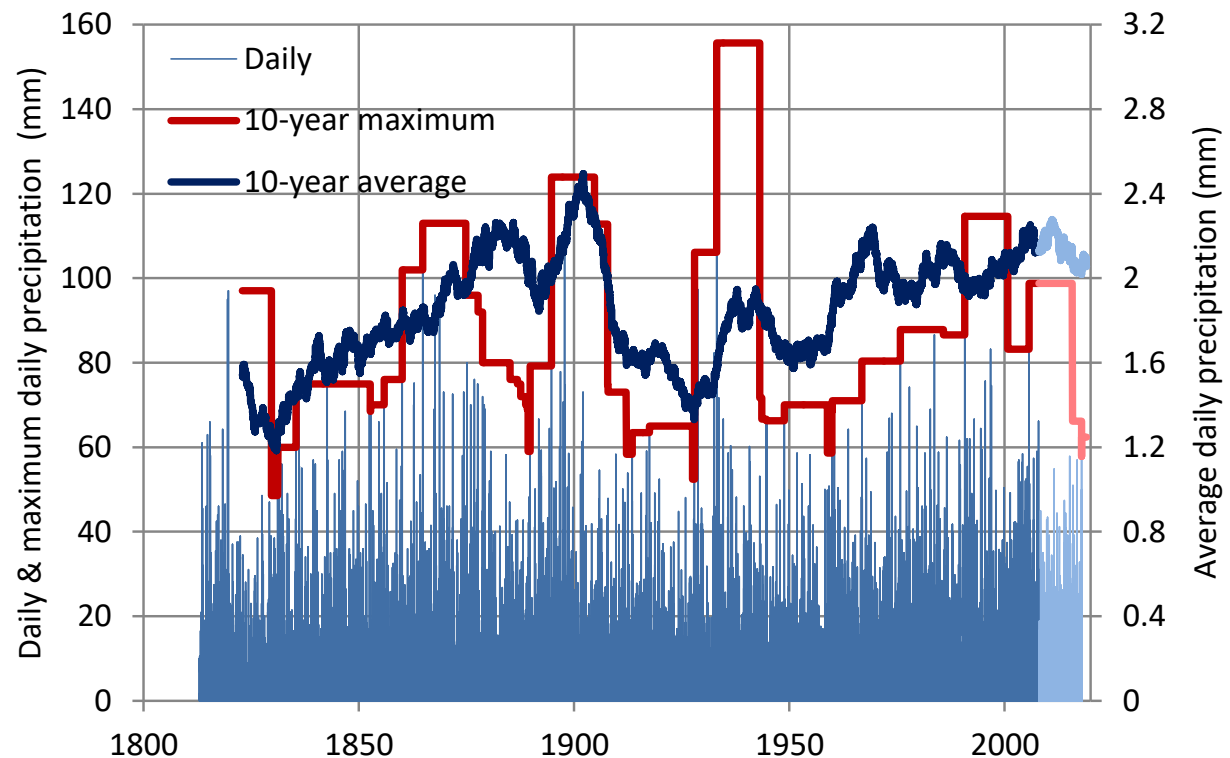
Total record length: 206 years.

Main observation:

The 10-year climatic averages have varied irregularly by a factor of 2 for the average daily precipitation and by a factor > 3 for the maximum daily precipitation.

Are “nonstationary” analyses and trend identification useful?

Author’s opinion: Such analyses are both fashionable and funny. But they are of little scientific value. Scientifically, they rather signify a step back.

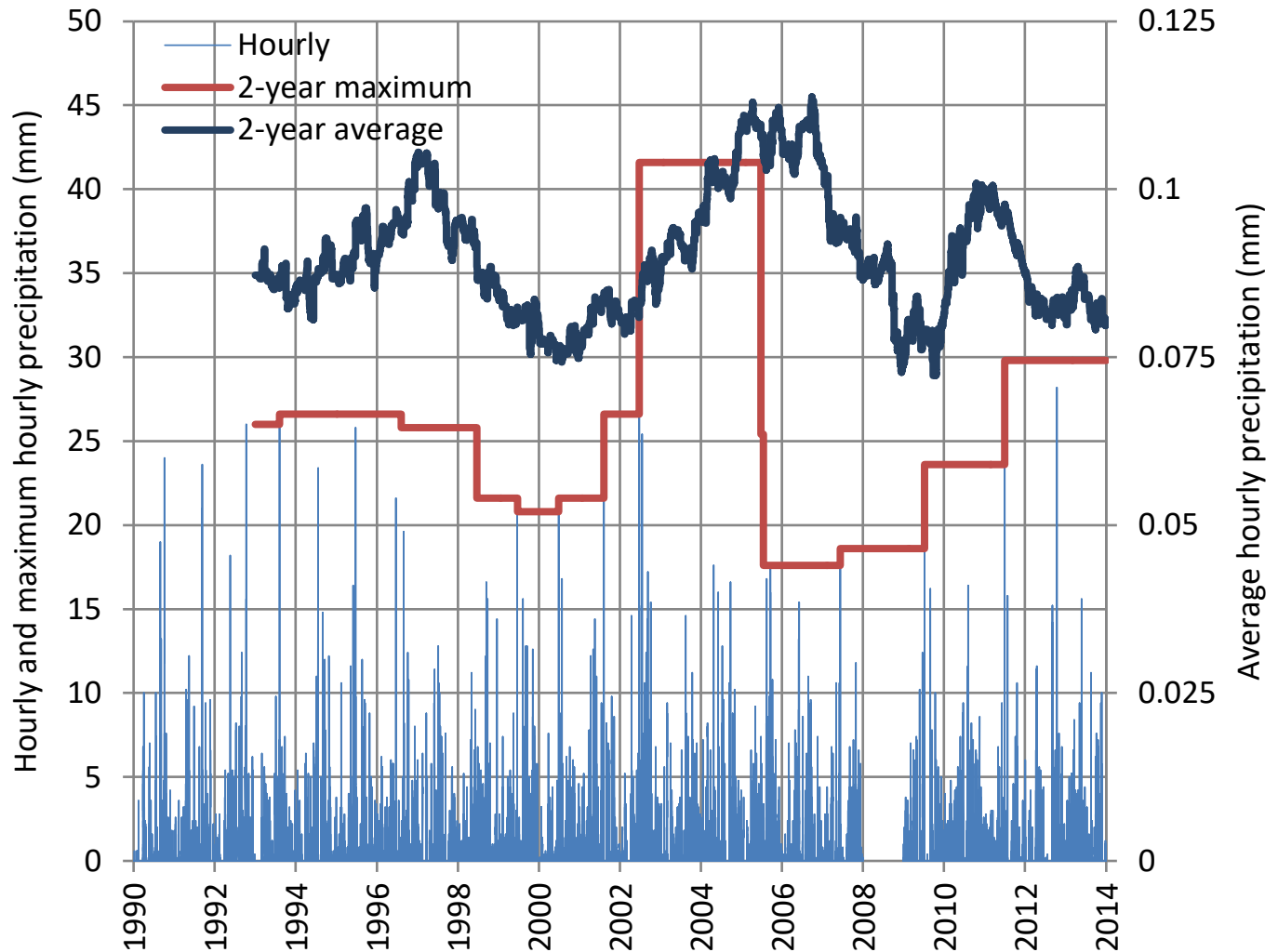


Data for illustration 2: Hourly precipitation in Bologna

Hourly rainfall data of the Bologna station for the period 1990-2013 are also available, provided by the Dext3r repository.

23 years full coverage, while the entire 2008 is missing (retrieved and processed by Lombardo et al., 2019).

Main observation:
Again we have fluctuations with upward and downward segments.

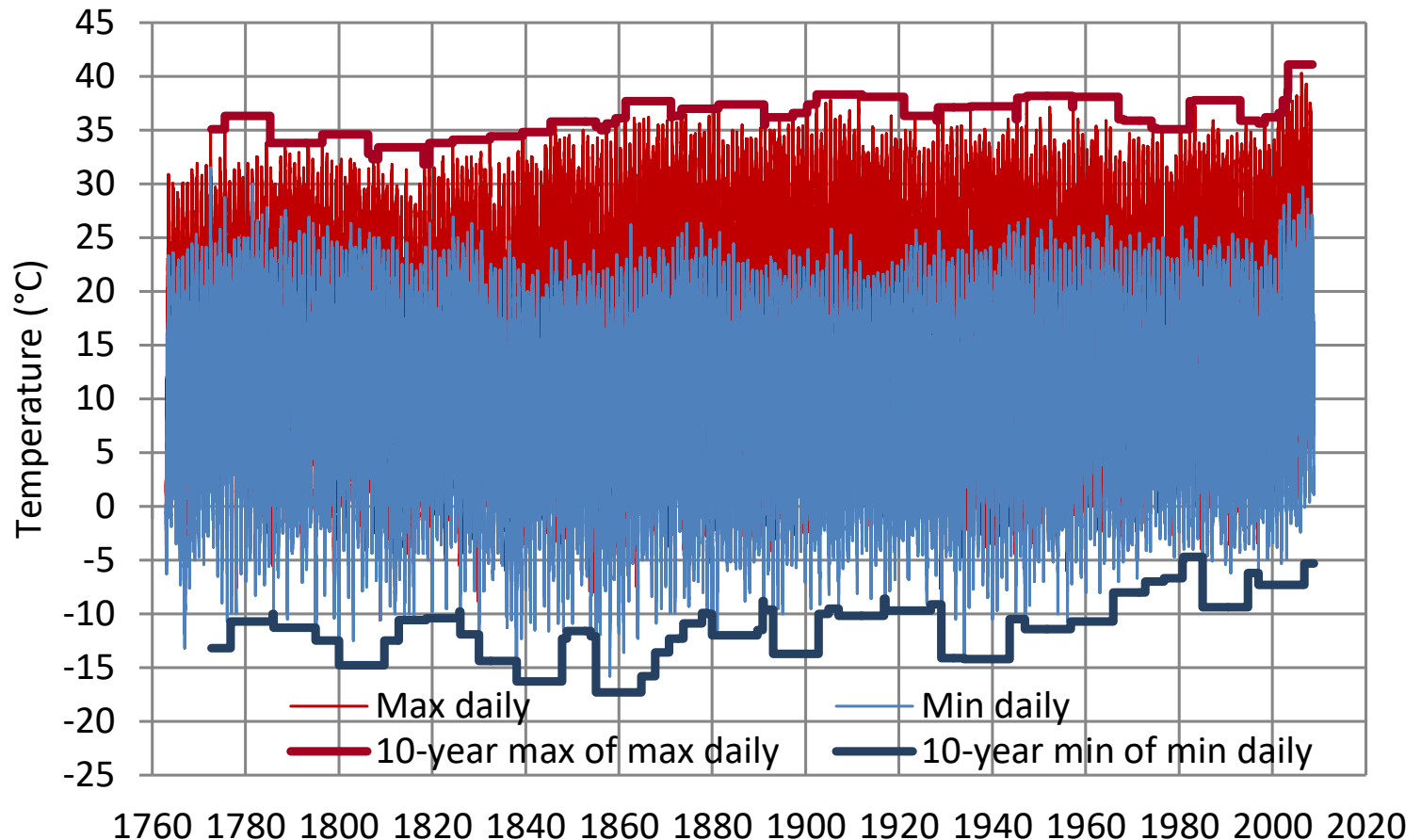


Data for illustration 3: Daily minimum and maximum temperature in Milan

Milano, Italy (45.47N, 9.19E,150.0m). Available from the Global Historical Climatology Network (GHCN) - Daily. Almost uninterrupted for the period 1763-2008: **246 years**.

Main observation:

Again we have upward and downward fluctuations; the upward ones prevail.



Introductory notes on statistical inference: moments

- Statistical inference (induction) is based on expectations of functions of stochastic variables, and in particular, moments, which are estimated from samples by virtue of stationarity and ergodicity.
- The **behaviour of extremes** is strongly related to **high-order moments**.
- The ergodic theorem enables, in theory, estimation of moments from data as $n \rightarrow \infty$, irrespective of the moment order p . But what happens for finite n ?
- It is recalled that the classical definitions of noncentral (or raw) and central moments of order p are:

$$\mu'_p := E[\underline{x}^p], \quad \mu_p := E[(\underline{x} - \mu)^p]$$

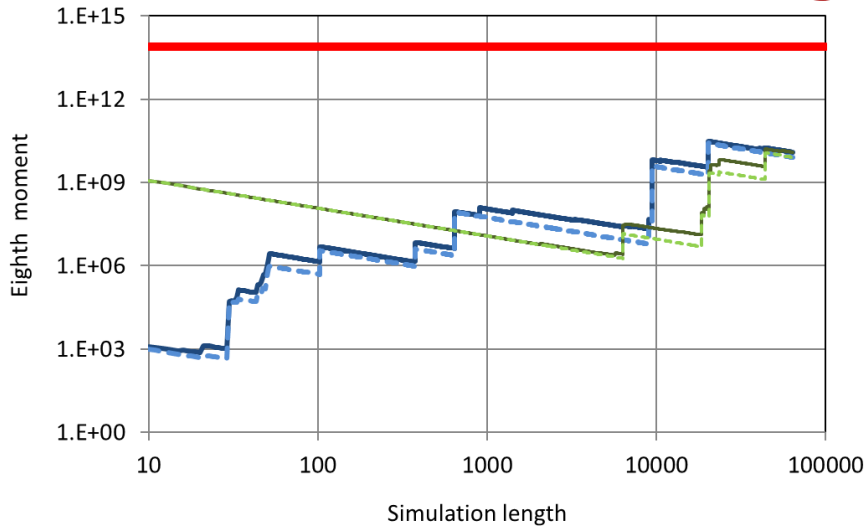
respectively, where $\mu := \mu'_1 = E[\underline{x}]$ is the mean of the stochastic variable \underline{x} . Their standard estimators from a sample $\underline{x}_i, i = 1, \dots, n$, are

$$\hat{\mu}'_p = \frac{1}{n} \sum_{i=1}^n \underline{x}_i^p, \quad \hat{\mu}_p = \frac{b(n, p)}{n} \sum_{i=1}^n (\underline{x}_i - \hat{\mu})^p$$

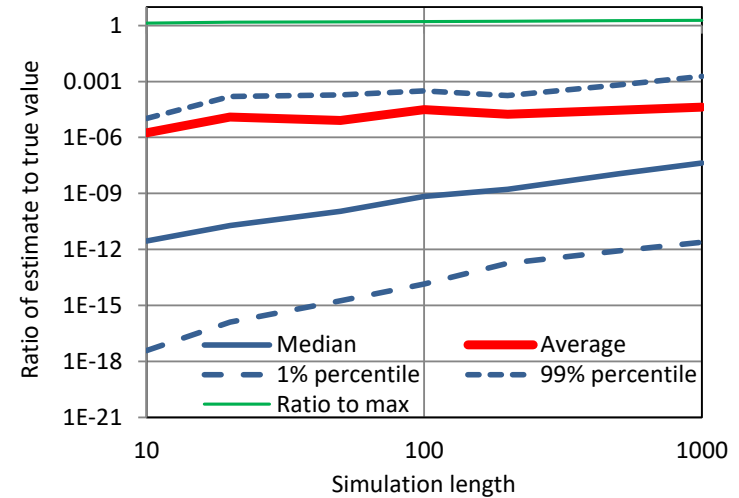
where $b(n, p)$ is a bias correction factor (e.g. for the variance $\mu_2 =: \sigma^2$, $b(n, 2) = n/(n - 1)$).

- The estimators of the noncentral moments $\hat{\mu}'_p$ are in theory unbiased, but in typical hydrological records it is practically impossible to use them in estimation for $p > 2$:
cf. Lombardo et al. (2014), “**Just two moments**”.
- For this reason in Koutsoyiannis (2019) the term “**unknowable**” was coined to describe this characteristic of classical moments.

Illustration of slow convergence of moment estimates



Convergence of the sample estimate of the eighth non-central moment to its true value (thick horizontal line) corresponding to a lognormal distribution $LN(0,1)$ where the process is an exponentiated Hurst-Kolmogorov process with Hurst parameter $H = 0.9$. The sample moments ($\sum_{i=1}^n x_i^p / n$ with $p = 8$; continuous lines), are estimated from a single simulation of length 64 000, subset to sample size n from 10 to 64 000, with the subsetting being done either from the beginning to the end or from the end to the beginning. Dashed lines represent maximum values $(\max_{1 \leq i \leq n} (x_i))^p / n$.



As in the example on the left but for 200 simulated series of length 1000 each. The sampling distribution of the eighth moment estimator $\sum_{i=1}^n \underline{x}_i^8 / n$ is visualized by the percentiles, the median and the average, plotted as ratios to the true value. Theoretically, the ratio should be 1, but it is smaller by many orders of magnitude, and the convergence to 1 is very slow. (The convergence of the average could also be achieved if we used millions of simulated series instead of 200). In contrast, the ratio to $(\max_{1 \leq i \leq n} (x_i))^8 / n$ is ≈ 1 .

The reason of slow convergence

- What is the result of **raising to a power and adding**, i.e. $\sum_{i=1}^n x_i^p$ – like in estimating moments?

Linear, $p = 1$	Pythagorean, $p = 2$	Cubic, $p = 3$	High order, $p = 8$
$3 + 4 = 7$	$3^2 + 4^2 = 5^2$	$3^3 + 4^3 = 4.5^3$	$3^8 + 4^8 \approx 4^8$
$3 + 4 + 12 = 19$	$3^2 + 4^2 + 12^2 = 13^2$	$3^3 + 4^3 + 12^3 = 12.2^3$	$3^8 + 4^8 + 12^8 \approx 12^8$

- Symbolically, for relatively large p the estimate of μ'_p is*:

$$\hat{\mu}'_p = \frac{1}{n} \sum_{i=1}^n x_i^p \approx \frac{1}{n} \left(\max_{1 \leq i \leq n} (x_i) \right)^p$$

- Thus, for an unbounded variable \underline{x} and for large p , we can conclude that $\hat{\mu}'_p$ is **more an estimator of an extreme quantity**, i.e., the n th order statistic (the largest) raised to power p , **than an estimator of μ'_p** .
- Thus, unless p is very small, μ'_p is an **unknowable quantity**: we cannot infer its value from a sample. **This is the case even if n is extraordinarily large!**
- Also, the various $\hat{\mu}'_p$ for different orders p are in fact deformed copies of the same thing: they only differ on the power to which the maximum value is raised.

* This is precise if x_i are positive. Note that for large p the term $(1/n)$ could be omitted with a negligible error.

From classical (but unknowable) moments to knowable moments

To derive **knowable** moments for high orders p , in the expectation defining the p th moment:

$$\mu'_p := E[\underline{x}^p]$$

we raise \underline{x} to a smaller power $q < p$ (e.g. $q = 1, q = 2$) and for the remaining $(p - q)$ terms in the multiplication $\underline{x}^p = \underbrace{\underline{x} \dots \underline{x}}_p$ we replace \underline{x} with the distribution function $F(\underline{x})$:

$$\underline{x}^p \rightarrow \left(F(\underline{x})\right)^{p-q} \underline{x}^q$$

We multiply the latter quantity by $(p - q + 1)$ and take its expected value. This leads to the following definition of **noncentral knowable moment**:

$$K'_{pq} := (p - q + 1)E \left[\left(F(\underline{x})\right)^{p-q} \underline{x}^q \right], \quad p \geq q$$

Likewise, we can define **central** and **hypercentral knowable moments** by the following substitutions:

$$(\underline{x} - \mu)^p \rightarrow \left(F(\underline{x})\right)^{p-q} (\underline{x} - \mu)^q \text{ or } (\underline{x} - \mu)^p \rightarrow (2F(\underline{x}) - 1)^{p-q} (\underline{x} - \mu)^q$$

Knowable moments or **K-moments**, introduced by Koutsoyiannis (2019, 2020), contain as special cases (or are one-to-one connected to) classical moments, Probability Weighted Moments and L-moments, and are tightly connected to expectations of order statistics.

Formal definition of K-moments

Noncentral knowable moment of order $(p, 1)$ [analogous to Probability Weighted Moments]

$$K'_p := pE \left[\left(F(\underline{x}) \right)^{p-1} \underline{x} \right], \quad p \geq 1$$

Noncentral knowable moment (or noncentral K-moment) of order (p, q) [recovering classical noncentral moments for $p = q$]:

$$K'_{pq} := (p - q + 1)E \left[\left(F(\underline{x}) \right)^{p-q} \underline{x}^q \right], \quad p \geq q$$

Central knowable moment of order (p, q) [recovering classical central moments for $p = q$]

$$K_{pq} := (p - q + 1)E \left[\left(F(\underline{x}) \right)^{p-q} (\underline{x} - \mu)^q \right], \quad p \geq q$$

where μ is the mean of \underline{x} , i.e., $\mu := E[\underline{x}_{(p)}] \equiv K'_1$.

Hypercentral knowable moment (or central K-moment) of order (p, q) [analogous to L-moments]

$$K_{pq}^+ := (p - q + 1)E \left[\left(2F(\underline{x}) - 1 \right)^{p-q} (\underline{x} - \mu)^q \right], \quad p \geq q$$

K-moments and order statistics

A **sample** of a stochastic variable \underline{x} is by definition a set $\{\underline{x}_1, \underline{x}_2, \dots, \underline{x}_n\}$ of independent copies of \underline{x} . We may arrange the sample in increasing order of magnitude such that $\underline{x}_{(i:n)}$ be the i th smallest of the n , i.e.:

$$\underline{x}_{(1:n)} \leq \underline{x}_{(2:n)} \leq \dots \leq \underline{x}_{(n:n)}$$

The stochastic variable $\underline{x}_{(i:n)}$ is termed the i th **order statistic**. The minimum and maximum are, respectively,

$$\underline{x}_{(1:n)} = \min(\underline{x}_1, \underline{x}_2, \dots, \underline{x}_n), \quad \underline{x}_{(n)} := \underline{x}_{(n:n)} = \max(\underline{x}_1, \underline{x}_2, \dots, \underline{x}_n)$$

and represent special cases of the order statistics, the lowest and the highest.

The distribution of the order statistic $\underline{x}_{(i:n)}$ is given in terms of the Beta distribution function as:

$$F_{(i:n)}(x) = P\{\underline{x}_{(i:n)} \leq x\} = P\{\underline{u} \leq F(x)\} = \frac{B_{F(x)}(i, n - i + 1)}{B(i, n - i + 1)}$$

For the special cases of the minimum and maximum we have, respectively,

$$F_{(1:n)}(x) = \frac{B_{F(x)}(1, n)}{B(1, n)} = 1 - (1 - F(x))^n, \quad F_{(n:n)}(x) = \frac{B_{F(x)}(n, 1)}{B(n, 1)} = (F(x))^n$$

It is shown that the expectation of the order statistic $\underline{x}_{(i:n)}$ is related to the noncentral K-moments by:

$$\frac{E[\underline{x}_{(i:n)}^q]}{i} = \binom{n}{i} \sum_{j=0}^{n-i} \binom{n-i}{j} (-1)^j \frac{K'_{i+j-1+q, q}}{i+j}$$

K-moments and expectation of extremes

Based on the definition of K-moments it is readily seen that

$$K'_p = E[\underline{x}_{(p)}] = E[\max(\underline{x}_1, \underline{x}_2, \dots, \underline{x}_p)]$$

More generally, K-moments of all categories represent expected values of extremes. Thus, for odd q or for nonnegative \underline{x} (so that \underline{x}_1^q be monotonic function of \underline{x}):

$$K'_{pq} = E[\max(\underline{x}_1^q, \underline{x}_2^q, \dots, \underline{x}_{p-q+1}^q)] = E[\underline{x}_{(p-q+1)}^q]$$

Furthermore, for odd q we have,

$$K_{pq} = E\left[\max\left((\underline{x}_1 - \mu)^q, (\underline{x}_2 - \mu)^q, \dots, (\underline{x}_{p-q+1} - \mu)^q\right)\right] = E\left[\left(\max(\underline{x}_1, \dots, \underline{x}_{p-q+1}) - \mu\right)^q\right]$$

which means that the central K-moment K_{pq} of \underline{x} is identical to the expected maximum of order $p - q + 1$ of $\underline{z} = (\underline{x} - \mu)^q$.

The above properties also hold asymptotically, for large p , also for even q in any case of positively skewed distribution.

For a symmetric distribution, an analogous property holds for the hypercentral moments with even q :

$$K_{pq}^+ = E\left[\max\left((\underline{x}_1 - \mu)^q, (\underline{x}_2 - \mu)^q, \dots, (\underline{x}_{p-q+1} - \mu)^q\right)\right]$$

which means that the hypercentral K-moment K_{pq}^+ of a stochastic variable \underline{x} with symmetrical distribution for q even is identical to the expected maximum of order $p - q + 1$ of \underline{z} . In contrast, for q odd, the hypercentral K-moment K_{pq}^+ will obviously be zero.

Are those high-order K-moments knowable?

Yes, because we can construct estimators with good properties such as unbiasedness, small variance and fast convergence to the true value.

The unbiased estimator of the noncentral moment K'_{p1} and its extension for $q > 1$ are (Koutsoyiannis, 2020):

$$\hat{K}'_p = \sum_{i=1}^n b_{inp} \underline{x}_{(i:n)}, \quad \hat{K}'_{pq} = \sum_{i=1}^n b_{i,n,p-q+1} \underline{x}_{(i:n)}^q$$

where for any positive number p (usually, but not necessarily, integer):

$$b_{inp} = \begin{cases} 0, & i < p \\ \frac{p}{n} \frac{\Gamma(n-p+1)}{\Gamma(n)} \frac{\Gamma(i)}{\Gamma(i-p+1)}, & i \geq p \geq 0 \end{cases}$$

It can be verified that

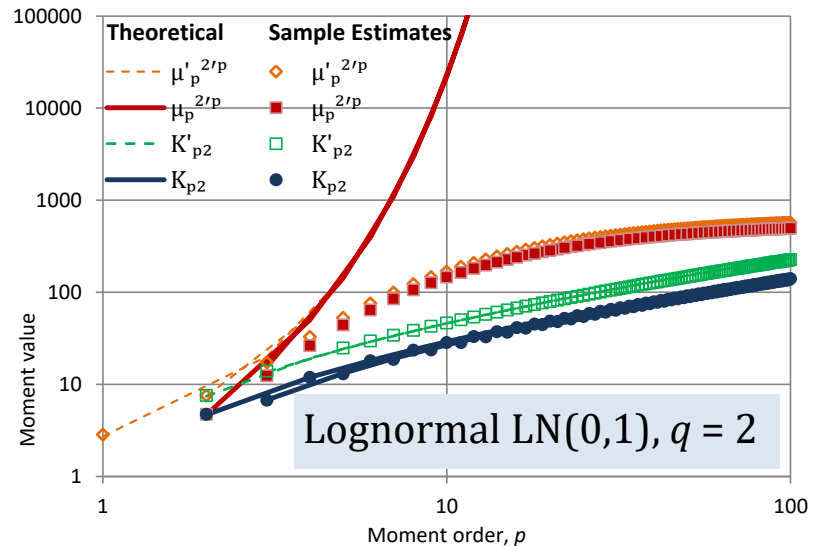
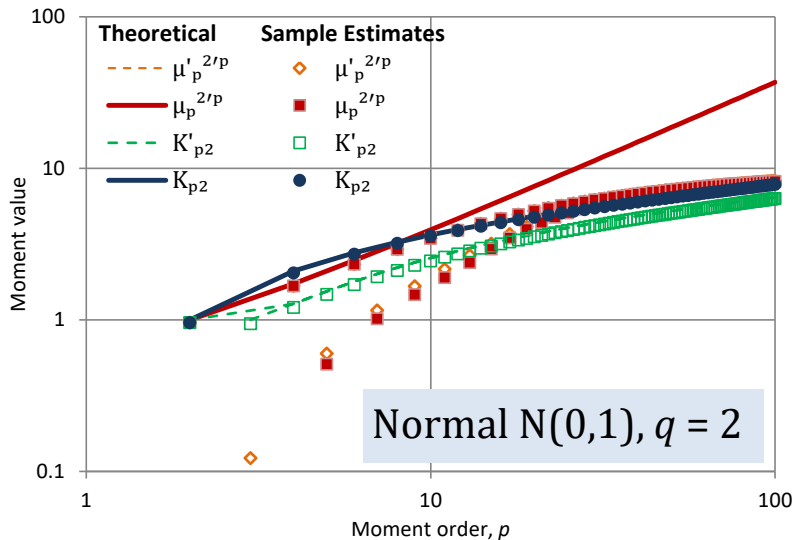
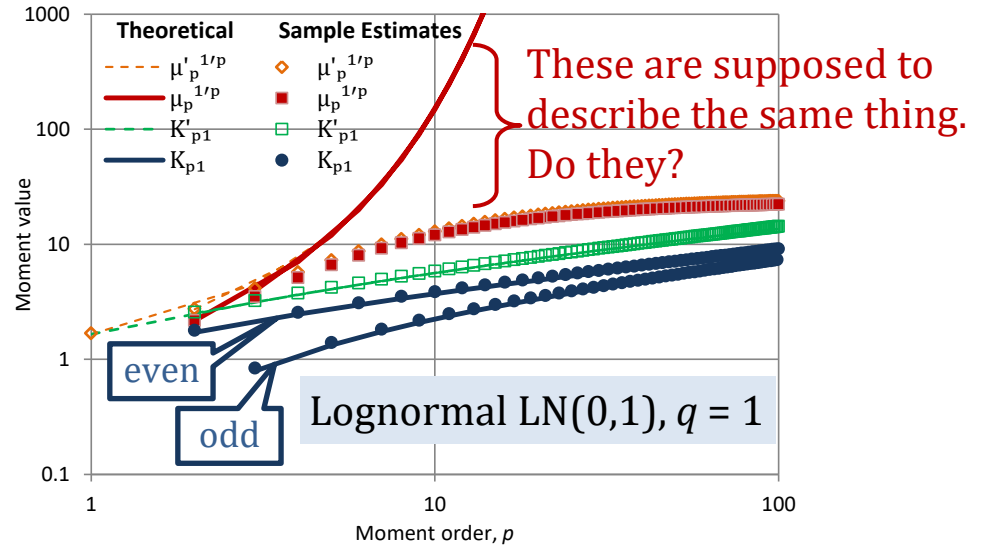
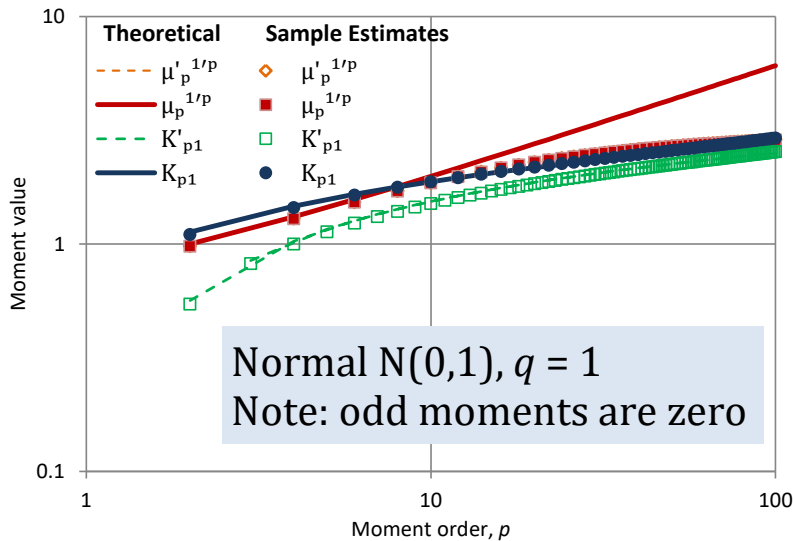
$$\sum_{i=1}^n b_{inp} = 1$$

which is a necessary condition for unbiasedness. Furthermore, for $p = 1$, $b_{in1} = 1/n$ and thus we recover the estimator of the mean. For $p = 2$, the quantity $(n/2)b_{in2}$ is the estimator $\hat{F}(x_{(i)})$, i.e.,

$$\hat{F}(x_{(i)}) = \frac{i-1}{n-1}$$

Because $b_{inp} = 0$ for $i < p$, as the moment order increases, progressively, fewer data values determine the moment estimate, until it remains only one, the maximum, when $p = n$, with $b_{nnn} = 1$. Furthermore, if $p > n$ then $b_{inp} = 0$ for all i , $1 \leq i \leq n$, and therefore estimation becomes impossible.

Justification of the notion of unknowable vs. knowable



Note: Sample sizes are ten times higher than the maximum p shown in graphs, i.e., 1000.

Effect of persistence on K-moment estimates

A K-moment is a characteristic of the marginal, first order, distribution of a process and therefore it is not affected by the dependence structure. However, its estimator is: time dependence induces bias to estimators of K-moments. Thus, the unbiasedness ceases to hold in stochastic processes.

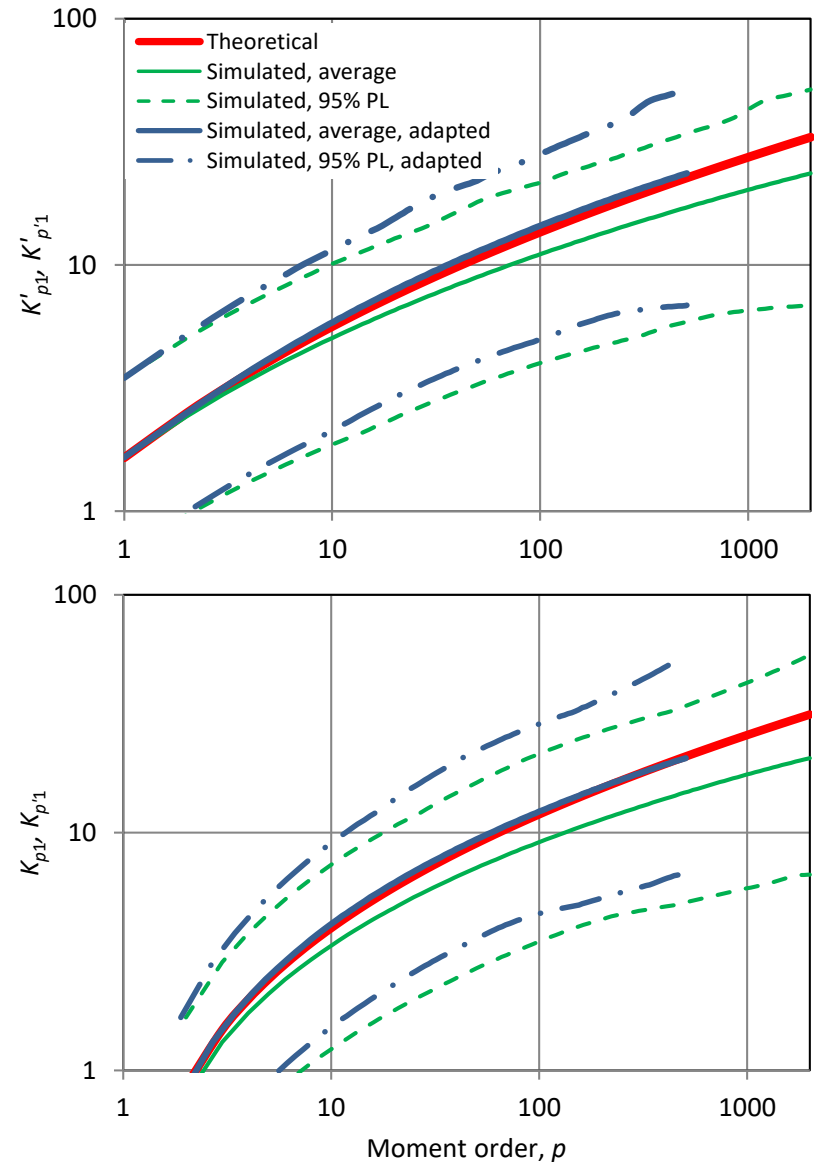
For a **Markov** process the effect of autocorrelation is **negligible**, unless n is low and r high (e.g. > 0.90).

However, for an **HK process**, as shown in Koutsoyiannis (2020), the effect can be **substantial**:

$$\Theta(n, H) = \frac{K_p^d - K_p}{K_p} \approx \frac{2H(1-H)}{n-1} - \frac{1}{2(n-1)^{2-2H}}$$

$$K_{p'} = K_p^d = (1 + \Theta)K_p, p' \approx 2\Theta + (1 - 2\Theta)p^{((1+\Theta)^2)}$$

Illustration of the performance of the adaptation of K-moment estimation for an HK process with Hurst parameter 0.9 and lognormal marginal distribution (LN(0,1)). Shown are noncentral and central moments, for $q = 1$. The estimates are averages of 200 simulations each with $n = 2000$ and are almost indistinguishable from the theoretical values. The 95% prediction limits (PL) are also shown. The maximum $p = 2000$ reduces $p' \approx 500$, i.e. to one fourth, with an analogous reduction to the return period.

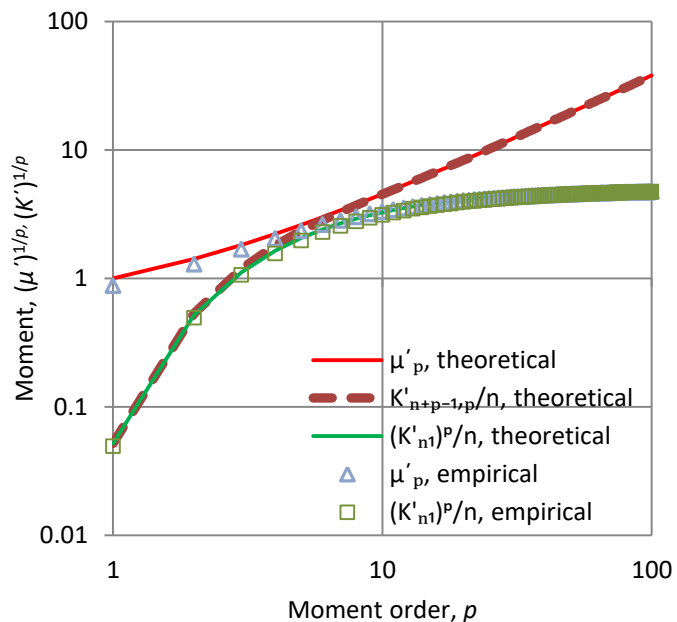
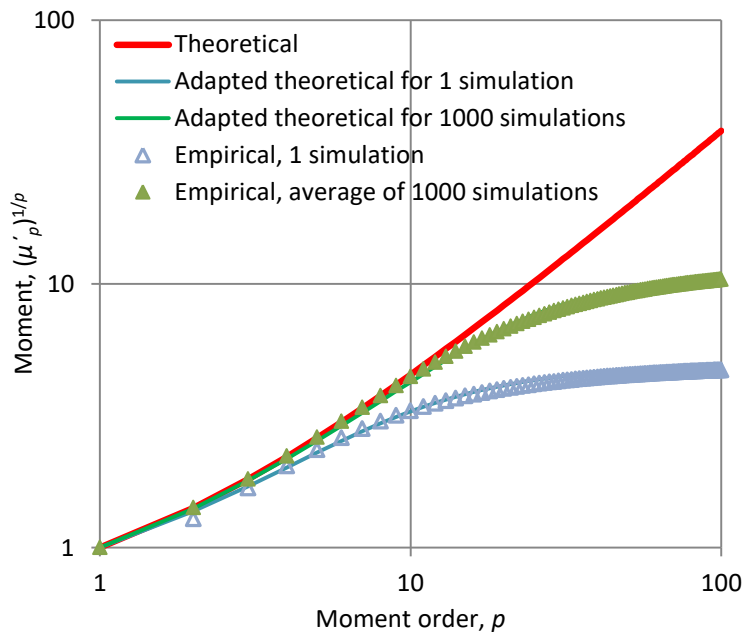


K-moments and classical moments

Not only are K-moments knowable but they can also predict the value that a classical moment estimator will give, through equation:

$$\hat{\mu}'_p \approx \frac{(K'_{mn,1})^p}{K'_{mn+p-1,p}} \mu'_p$$

where n is the sample size and m is the number of samples for the case where more than one sample are available to make the estimate.



(Left) Comparison of the estimates of classical noncentral moments from 1 and 1000 independent samples from the exponential distribution to (a) the theoretical moments and (b) to the values determined by the above equation (adapted theoretical). (Right) Additional information of the terms appearing in the above equation.

K-moments and classical moments (2)

- Generally, as p becomes large approaching n , **estimates** of both **classical and K-moments, central or non-central, become estimates of expressions involving extremes** such as $(\max_{1 \leq i \leq p} x_i)^q$ or $\max_{1 \leq i \leq p} (x_i - \mu)^q$.
- For the K-moments this is consistent with their theoretical definition. For the classical moments this is an inconsistency.
- A common property of both central classical moments and hypercentral K-moments is that symmetrical distributions have all their odd moments equal to zero.
- For unbounded variables both classical and K moments are non-decreasing functions of p , separately for odd and even p .
- **In geophysical processes we can justifiably assume that the variance $\mu_2 \equiv \gamma_1 \equiv \sigma^2 \equiv K_{22}$ is finite** (an infinite variance would presuppose infinite energy to materialize, which is absurd). Hence, **high order K-moments K_p and K_{p2} are finite** too, even if classical moments μ_p diverge to infinity beyond a certain p (i.e., in heavy tailed distributions).

K-moments and L-moments

Hypercentral K-moments are virtually equivalent to L-moments for small orders. In addition, the framework of K-moments provides alternative options to define summary statistical characteristics of the distribution, including the classical ones, as in the table below. (Which option is preferable depends on the statistical behaviour, and in particular, the mean, mode and variance, of the estimator.)

Characteristic	Order p	Option 1	Option 2	Option 3*
Location	1	$K'_{11} = \mu$ (the classical mean)		
Variability	2	$K_{21}^+ = 2K_{21} = 2(K'_{21} - \mu) = 2\lambda_2$	$K_{22}^+ = K_{22} = \mu_2 = \sigma^2$ (the classical variance)	
Skewness (dimensionless)	3	$\frac{K_{31}^+}{K_{21}^+} = 2\frac{K_{31}}{K_{21}} - 3 = \frac{\lambda_3}{\lambda_2}$	$\frac{K_{32}^+}{K_{22}^+} = 2\frac{K_{32}}{K_{22}} - 2$	$\frac{K_{33}}{K_{22}^{3/2}} = \frac{\mu_3}{\sigma^3}$
Kurtosis (dimensionless)	4	$\frac{K_{41}^+}{K_{21}^+} = 4\frac{K_{41}}{K_{21}} - 8\frac{K_{31}}{K_{21}} + 6 = \frac{4\lambda_4}{5\lambda_2} + \frac{6}{5}$	$\frac{K_{42}^+}{K_{22}^+} = 4\frac{K_{42}}{K_{22}} - 6\frac{K_{32}}{K_{22}} + 3$	$\frac{K_{44}}{K_{22}^2} = \frac{\mu_4}{\sigma^4}$

However, the real power of K-Moments is in their determination and use for very high orders p , up to the sample size.

High order moments for stochastic processes at different time scales: the K-climacogram and the K-climacospectrum

- The full description of the third-order, fourth-order, etc., properties of a stationary stochastic process requires functions of 2, 3, ..., variables.
- For example, the **third order properties are expressed in terms of a function of two lags**:

$$c_3(h_1, h_2) := E[(\underline{x}(t) - \mu) (\underline{x}(t + h_1) - \mu) (\underline{x}(t + h_2) - \mu)]$$

- Such a description is **not parsimonious and its accuracy holds only in theory**, because sample estimates are not reliable.
- This problem is remedied if we **introduce single-variable descriptions for any order p** , expanding the idea of the climacogram and climacospectrum based on K-moments.

$$\text{K-climacogram: } \gamma_{pq}(k) = (p - q + 1)E\left[\left(2F(\underline{X}(k)/k) - 1\right)^{p-q} (\underline{X}(k)/k - \mu)^q\right]$$

$$\text{K-climacospectrum: } \zeta_{pq}(k) = \frac{k \left(\gamma_{pq}(k) - \gamma_{pq}(2k) \right)}{\ln 2}$$

where $\underline{X}(k) := \int_0^k \underline{x}(t)dt$ is the cumulative process, and $\underline{X}(k)/k$ is the time averaged process at time scale k .

- For $p = q = 2$ we obtain the standard climacogram, $\gamma_{22}(k) \equiv \gamma(k)$, and the standard climacospectrum, $\zeta_{22}(k) \equiv \zeta(k)$.

Assigning return periods to K-moments of any order

- The non-central K-moment for $q = 1$ is $K'_p = pE \left[\left(F(\underline{x}) \right)^{p-1} \underline{x} \right]$
- By definition, it represents the expected value of the maximum of p copies of \underline{x} .
- To determine the theoretical return period $T(K'_p)$ we introduce the ratio Λ_p which happens to vary only slightly with p ; assuming a time unit D we have:

$$T(K'_{p1}) = \frac{D}{1 - F(K'_{p1})}, \quad \Lambda_p := \frac{T(K'_{p1})}{D p} = \frac{1}{p(1 - F(K'_{p1}))}$$

- Any symmetric distribution will give exactly $\Lambda_1 = 2$ because K'_1 is the mean, which equals the median and thus has a return period of $2D$. Thus, a rough approximation is the rule of thumb:

$$\Lambda_p \approx 2$$

- Generally, the exact value Λ_1 is easy to determine, as it is the return period of the mean:

$$\Lambda_1 = \frac{1}{1 - F(\mu)} = \frac{T(\mu)}{D}$$

- The exact value of Λ_∞ depends only on the tail index ξ of the distribution:

$$\Lambda_\infty = \begin{cases} \Gamma(1 - \xi)^{\frac{1}{\xi}}, & \xi \neq 0 \\ e^\gamma, & \xi = 0 \end{cases}$$

where $\gamma = 0.577$ is the Euler's constant.

- These enable the simple approximation of Λ_p and hence of the return period:

$$\Lambda_p \approx \Lambda_\infty + (\Lambda_1 - \Lambda_\infty)(1/p), \quad T(K'_p)/D = p\Lambda_p \approx \Lambda_\infty p + (\Lambda_1 - \Lambda_\infty)$$

Better approximation of the relationship between p and T

- An almost perfect approximation of Λ_p for any distribution function is:

$$\Lambda_p \approx \Lambda_\infty + \left(\Lambda_1 - \Lambda_\infty - B \ln \left(1 + \frac{\beta}{2^\beta - 1} \right) \right) \frac{1}{p} + B \ln \left(1 + \frac{\beta}{(p+1)^\beta - 1} \right)$$

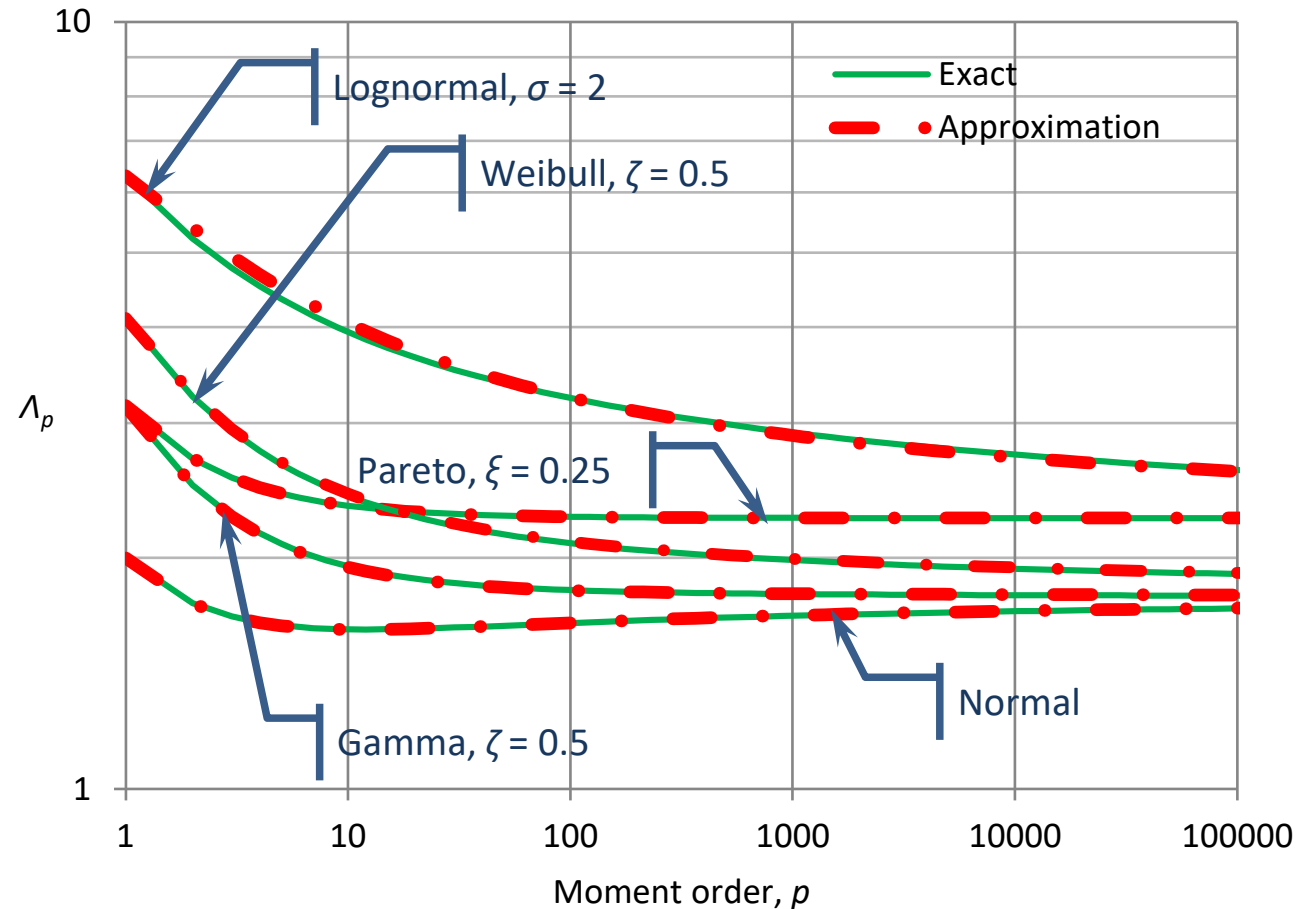
- This involves two constants β and B , which depend on the distribution function.

- For example, in the Pareto distribution, $\beta = 1$ and

$$B = \frac{(3 - \xi)\Lambda_\infty - 2\Lambda_1}{2(1 - \ln 2)}$$

- For parameters of other distributions see Koutsoyiannis (2020).

- The graph indicates the perfect agreement of the approximation to the exact values for several distributions.



Assigning return periods to order statistics (plotting positions)

The classical formula for assigning a return period to $x_{(i:n)}$, i.e., the i th smallest value in a sample of size n is:

$$\frac{T_{(i:n)}}{D} = \frac{n + B}{n - i + A}$$

where A and B are constants. For an unbiased estimate of the distribution quantile these constants are $A = 1/\Lambda_\infty$, $B = \Lambda_1/\Lambda_\infty - 1$ (Koutsoyiannis, 2020) and thus

$$\frac{T_{(i:n)}}{D} = \frac{\Lambda_\infty(n - 1) + \Lambda_1}{\Lambda_\infty(n - i) + 1}$$

For the highest value $x_{(n)} \equiv x_{(n:n)}$ both approaches, K-moments and order statistics, result in precisely the same value, $T(K'_n)/D = T_{(n:n)}/D = \Lambda_\infty p + (\Lambda_1 - \Lambda_\infty)$.

For smaller i , the p th K-moment should be equivalent, in terms of the corresponding return period, if

$$p = \frac{n - (\Lambda_1 - \Lambda_\infty)(n - i)}{\Lambda_\infty(n - i) + 1}$$

This means that:

- (a) $x_{(i:n)}$ can be used as a quick-and-dirty (QAD) estimate of K'_p , provided that p is given as a function of i from the above equation.
- (b) The return period estimate based on the typical estimator $\hat{K}'_p = \sum_{i=1}^n b_{inp} x_{(i:n)}$ is better than that based on a single $x_{(i:n)}$ because it is derived from many data points (except for the maximum value, when $i = n$, where the two approaches are precisely identical).

Comparison of return periods assigned by the two approaches

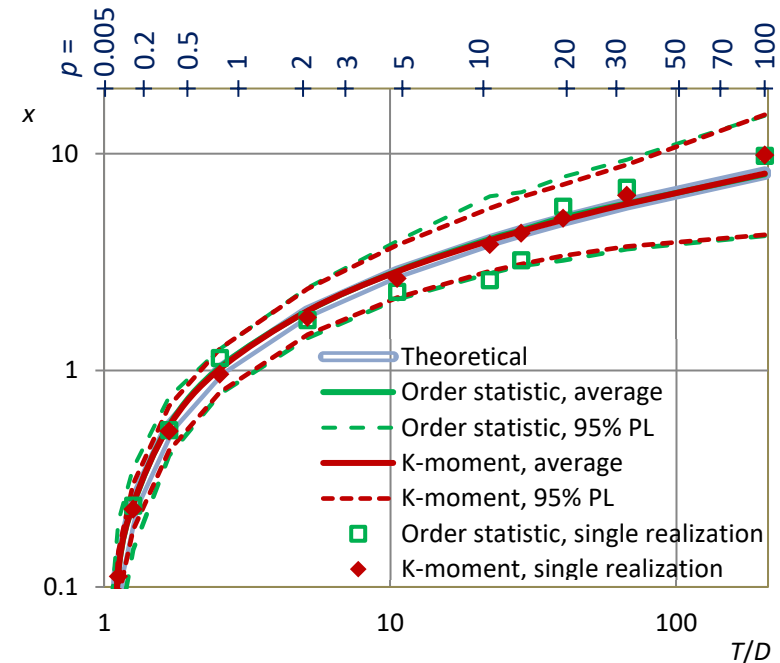
We assume a Pareto distribution with $\xi = 0.15$, in which $\Lambda_\infty = 2.035$ and $\Lambda_1 = 2.955$, and a sample of $n = 100$. We will have the following values of T and p for the highest and the second highest values:

i	$T_{(i:n)}$	p
100	204.4	100
99	67.4	32.6

Hence the estimate of the x quantile corresponding to a return period of 67.4, will be equal to:

- $x_{(99:100)}$ according to the order-statistics approach (the estimate is based on one data point);
- $\hat{K}'_{32.6}$ according to the K-moments approach (the estimate is based on 68 data points and will be a weighted average of $x_{(i:100)}$ for $i = 33$ to $i = 100$).

Simulation results of empirical return periods assigned to Pareto quantiles (for tail index $\xi = 0.15$, scale parameter $\lambda = 1$ and lower bound zero). Averages and prediction limits (PL) were calculated from 200 simulations each with $n = 100$. The curves of averages for both the order statistics and the K-moment approaches are indistinguishable from the theoretical curves. The return periods were assigned for the unbiased quantile option. The correspondence between the K-moment of order p and the return period T is also shown through the upper horizontal axis. The plots of a single realization are also shown (but for part of the empirical points to avoid an overcrowded graph).



Very high order K-moments relationships between p and T

From the relationship:

$$p = \frac{T}{\Lambda_{\infty} D} - \frac{\Lambda_1}{\Lambda_{\infty}} + 1,$$

we can easily find the K-moment order p corresponding to the return period T . An example is given in the following table:

<i>Example of the K-moment order p corresponding to the specified return period for the Pareto distribution with shape parameter $\xi = 0.15$.</i>			
	$D = 10 \text{ min}$	$D = 1 \text{ h}$	$D = 1 \text{ d}$
$T = 2 \text{ months}$	4 307	717	29
$T = 1 \text{ year}$	25 842	4 307	179
$T = 2 \text{ years}$	51 684	8 614	358
$T = 100 \text{ years}$	2 584 212	430 702	17 945

In a stochastic process with dependence, what is given in the table is the adapted moment order p' while p should be estimated from p' based on the relationship in p. 25.

Alternatively, the more accurate approximation of p. 31 or even the exact relationships could be used but the resulting p will not differ substantially from the above values.

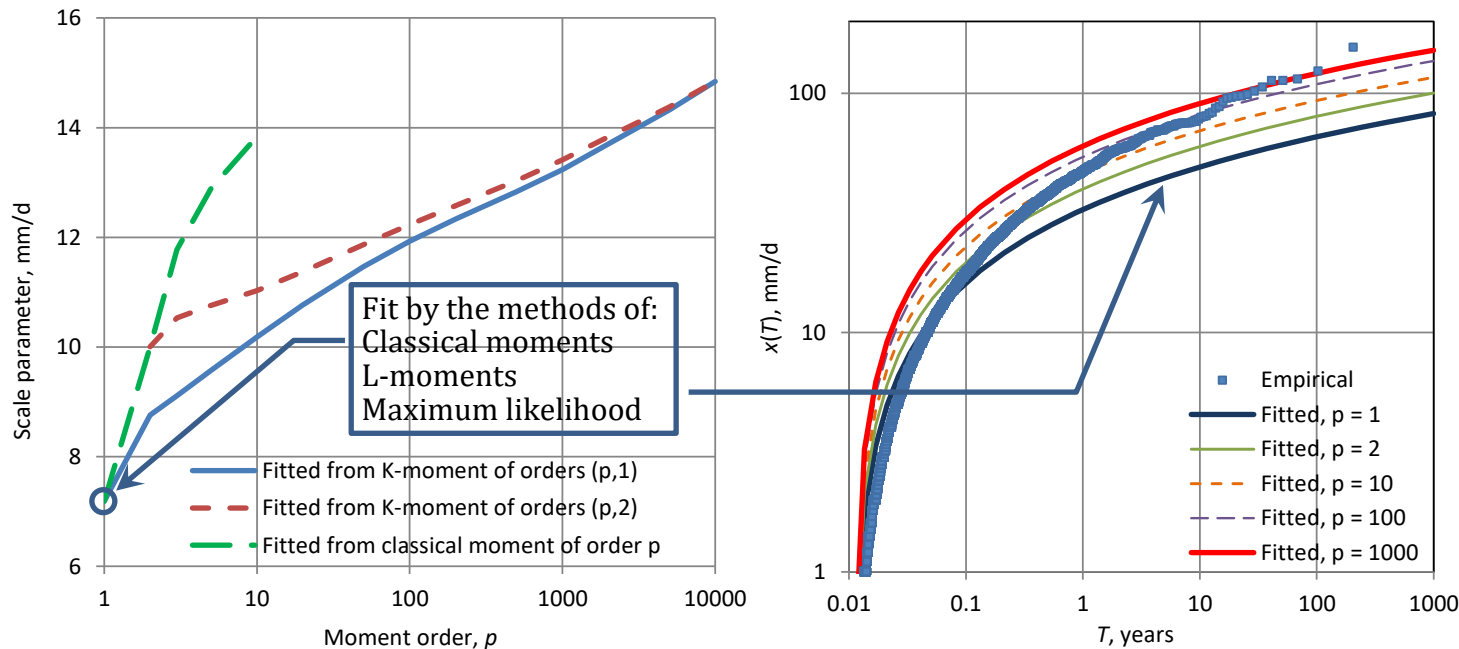
K-moments of such high order are reliably estimated.

Illustration that high-order K-moments are preferable to low-order moments

For the sake of illustration, for the daily rainfall in Bologna, we intentionally choose the simplest and blatantly unsuitable model, the 1-parameter exponential distribution, $F(x) = 1 - e^{-x/\lambda}$.

One moment suffices to estimate the single (scale) parameter λ —but which moment to choose?

The exact K-moments are: $K_{p1} = (H_p - 1)\lambda$, $K_{p2} = \left((H_{p-1} - 1)^2 + H_{p-1}^{(2)} \right) \lambda^2$, $K_{pp} = \mu_p = (!p)\lambda^p$, where H_p is the p th harmonic number and $H_p^{(2)}$ is the p th harmonic number of order 2.



The moment order p affects the fitting dramatically.
The scale parameter λ increases with increasing p, q .
If we wish to model maxima, it is better to fit based on the 1000th K-moment than on the 1st!

Better fitting on K-moments for orders p from ~ 100 to $10\,000$ ($T = \sim 2$ to 200 years)

We assume Pareto distribution with zero lower bound (for physical consistency):

$$F(x) = 1 - (1 + \xi x/\lambda)^{-\frac{1}{\xi}} \text{ or}$$

$$\frac{T(x)}{D} = (1 + \xi x/\lambda)^{\frac{1}{\xi}}$$

The exact relationship of K-moments with return period is:

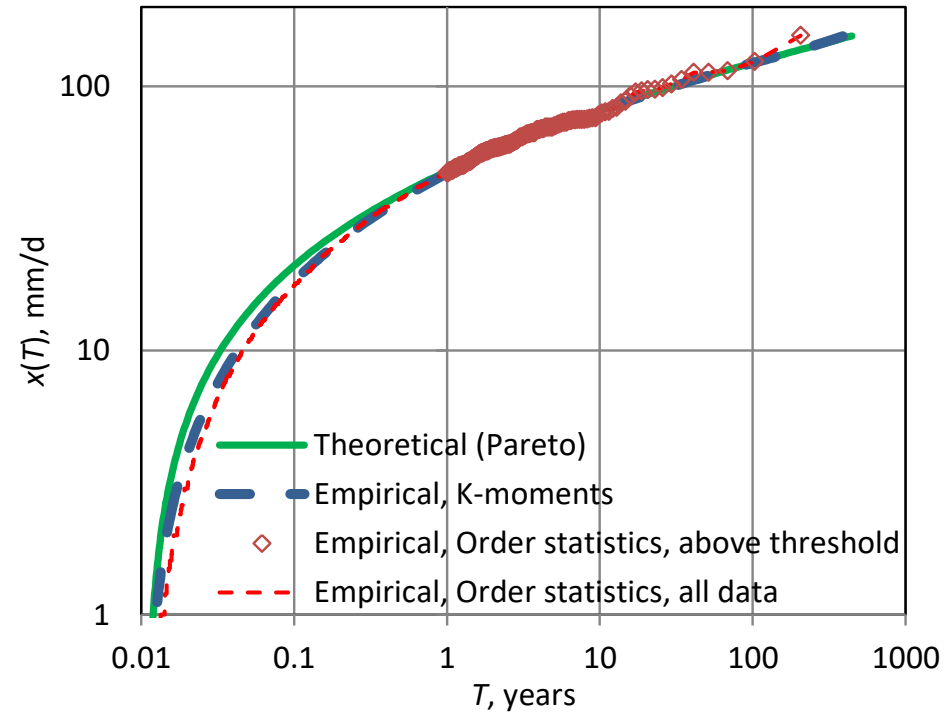
$$\frac{\hat{T}(\hat{K}'_p)}{D} = p\Lambda_p = ((p + 1 - \xi) B(1 - \xi, p + 1))^{\frac{1}{\xi}}$$

We estimate the parameters by minimizing the mean square error of the logarithms of the empirical $\hat{T}(\hat{K}'_p)$ from the theoretical $T(\hat{K}'_p)$. We calculate the error for a range of T from 2 to 200 years. The fitted parameters are $\xi = 0.096$, $\lambda = 8.37$ mm/d.

The graph shows a perfect fit of theoretical and empirical curves for $T > 1$ year (the two curves are indistinguishable).

For comparison, empirical curves for order statistics are also plotted (Weibull plotting positions).

Note: Minimizing the error of \hat{K}'_p with respect to K'_p , without reference to T , is another possibility but presupposes exact relationships for K'_p , which in other distributions may be infeasible to derive.



Slight improvement for a global fitting

By adding one parameter to the theoretical distribution function we can get a model applicable for the entire range of rainfall depth.

Namely, we use the Pareto-Burr-Fuller (PBF) distribution with zero lower bound (for physical consistency for rainfall):

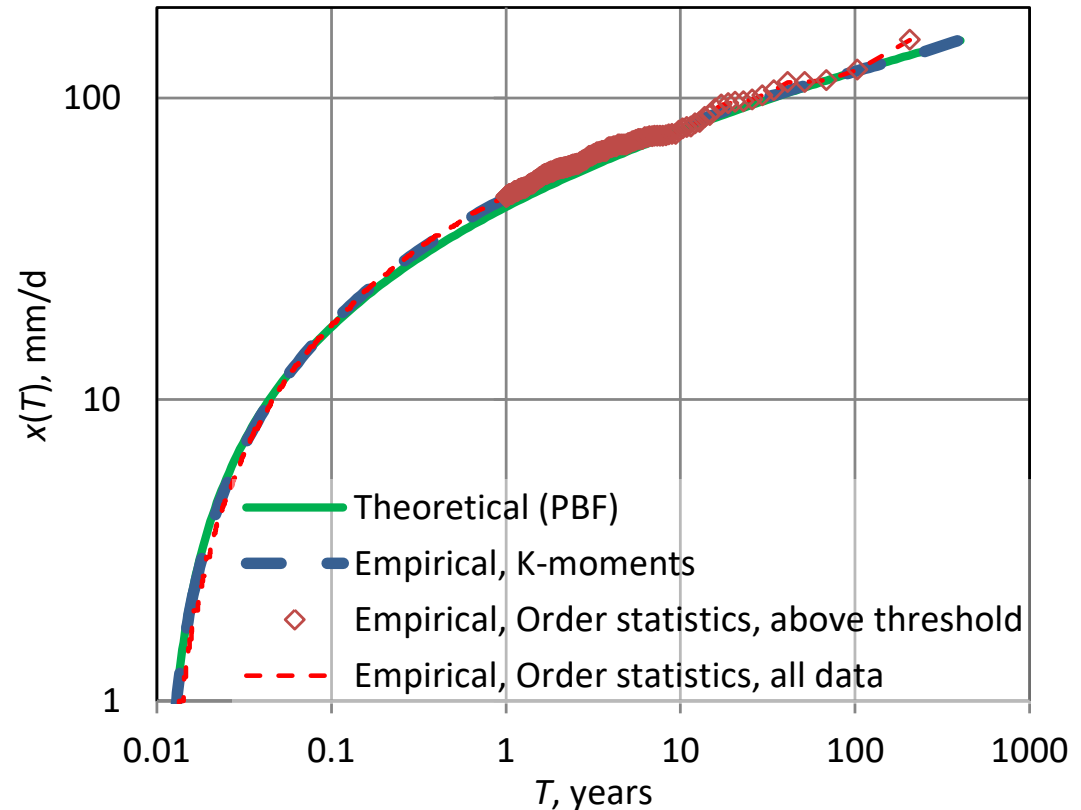
$$F(x) = 1 - \left(1 + \kappa(x/\lambda)^\zeta\right)^{-\frac{1}{\zeta\xi}}$$

We use the same estimation procedure as above but calculate the error on the entire range of values.

The estimated parameters are: $\xi = 0.096$, $\zeta = 0.883$, $\lambda = 5.04$ mm/d.

A perfect fit of the model (green continuous line) and empirical curve (blue dashed line) is seen for the entire range.

For comparison, empirical curves for order statistics are also plotted (Weibull plotting positions).



Ombrian model: Marginal distribution of rainfall intensity

An ombrian model (from the Greek ombros, meaning rainfall) describes the stochastic properties of the distribution of rainfall of any order, or equivalently, at any time scale.

From an ombrian model that is simple enough, the ombrian relationships, also known with the misnomer rainfall intensity – duration [meaning time scale] – frequency [meaning return period] curves are directly extracted. The assumptions of the proposed ombrian model follow.

1. Pareto distribution with discontinuity at the origin for small time scales:

$$F^{(k)}(x) = 1 - P_1^{(k)} \left(1 + \xi \frac{x}{\lambda(k)} \right)^{-1/\xi}$$

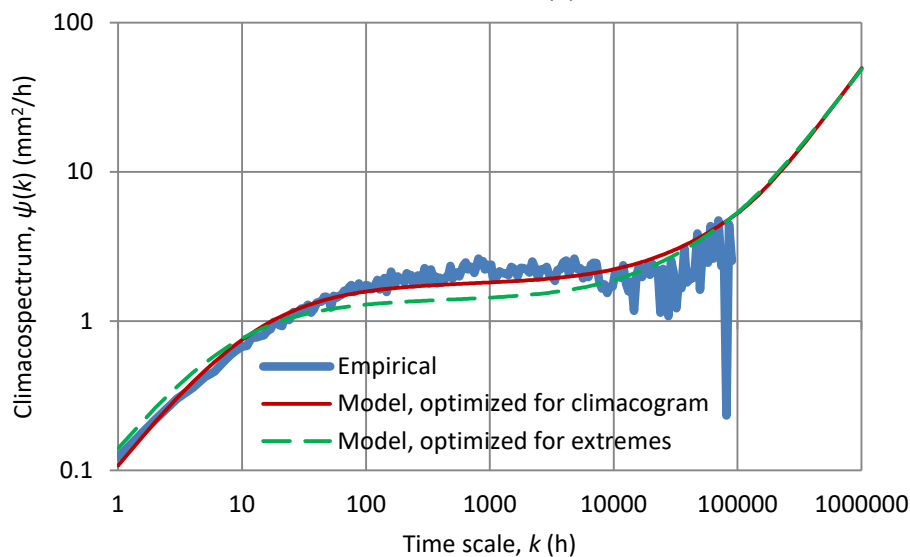
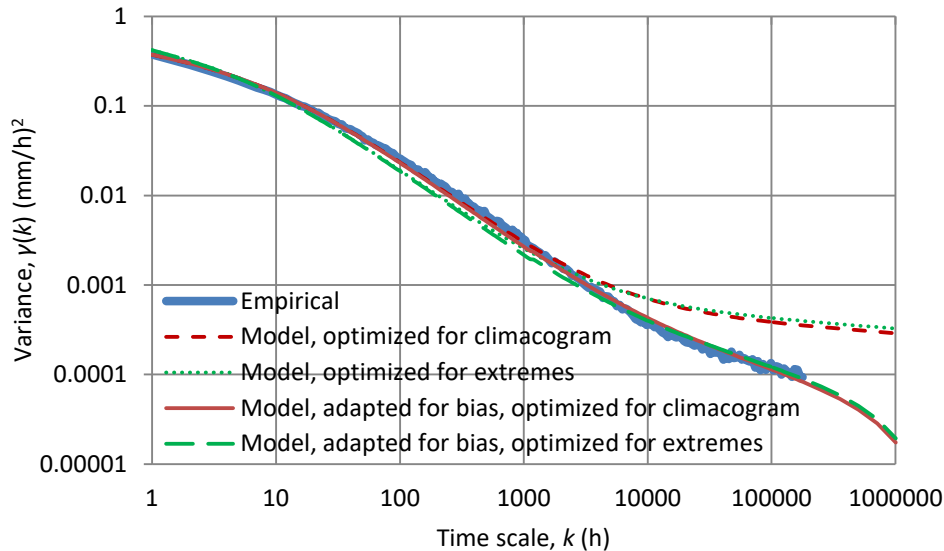
It is shown by theoretical reasoning (Koutsoyiannis, 2020) that the tail index ξ should be constant, while the probability wet, $P_1^{(k)}$, and the state scale parameter, $\lambda(k)$, are functions of the time scale k . Here we sacrifice the exactness of the PBF distribution (see previous page) in order to get simpler ombrian relationships for small scales.

2. Continuous PBF distribution with possible discontinuity at zero for large time scales, i.e.:

$$F^{(k)}(x) = 1 - P_1^{(k)} \left(1 + \xi \left(\frac{x}{\lambda(k)} \right)^{\zeta(k)} \right)^{-1/\xi}$$

In this case a new parameter $\zeta(k)$ is introduced, which is again a function of time scale. The Pareto distribution is a special case of PFB for $\zeta(k) = 1$. In contrast to the Pareto distribution, whose density is a decreasing function of x , the PBF tends to be bell-shaped for increasing $\zeta(k)$. Here we sacrifice the constancy of tail index ($= \xi/\zeta(k)$) to assure simplicity and ergodicity.

Ombrian model: Mean and climacogram



3. Constant mean of the time averaged process:

$$E[\underline{x}^{(k)}] = \mu$$

4. Climacogram of Filtered Hurst-Kolmogorov - Cauchy (FHK-C) type, i.e.:

$$\text{var}[\underline{x}^{(k)}] = \gamma(k) = \lambda_1 \left(1 + \left(\frac{k}{\alpha} \right)^{2M} \right)^{\frac{H-1}{M}}$$

or of Filtered Hurst-Kolmogorov - Cauchy-Dagum (FHK-CD) type; in the latter case, to avoid an overparametrized model (and as we expect $H > 0.5$ and $M < 0.5$ due to roughness), we set $M = 1 - H$ and thus we get:

$$\gamma(k) = \lambda_1 \left(1 + \frac{k}{\alpha_1} \right)^{2H-2} + \lambda_2 \left(1 - \left(1 + \frac{\alpha_2}{k} \right)^{2H-2} \right)$$

Clearly, in both cases, $\gamma(k) \rightarrow 0$, as $k \rightarrow \infty$, which makes the process ergodic; for $k = 0$, $\gamma(0) = \gamma_0 = \lambda$ in the FHK-C case and $\gamma(0) = \gamma_0 = \lambda_1 + \lambda_2$ in the FHK-CD case. In both cases $\gamma(0)$ is finite and the number of parameters is four.

The ombrian model: Probability wet/dry

5. Probability wet and dry, $P_1^{(k)} = 1 - P_0^{(k)}$, varying with time scale according to:

$$\ln P_0^{(k)} = \ln P_0^{(k^*)} (k/k^*)^\theta, \quad k \geq k^*$$

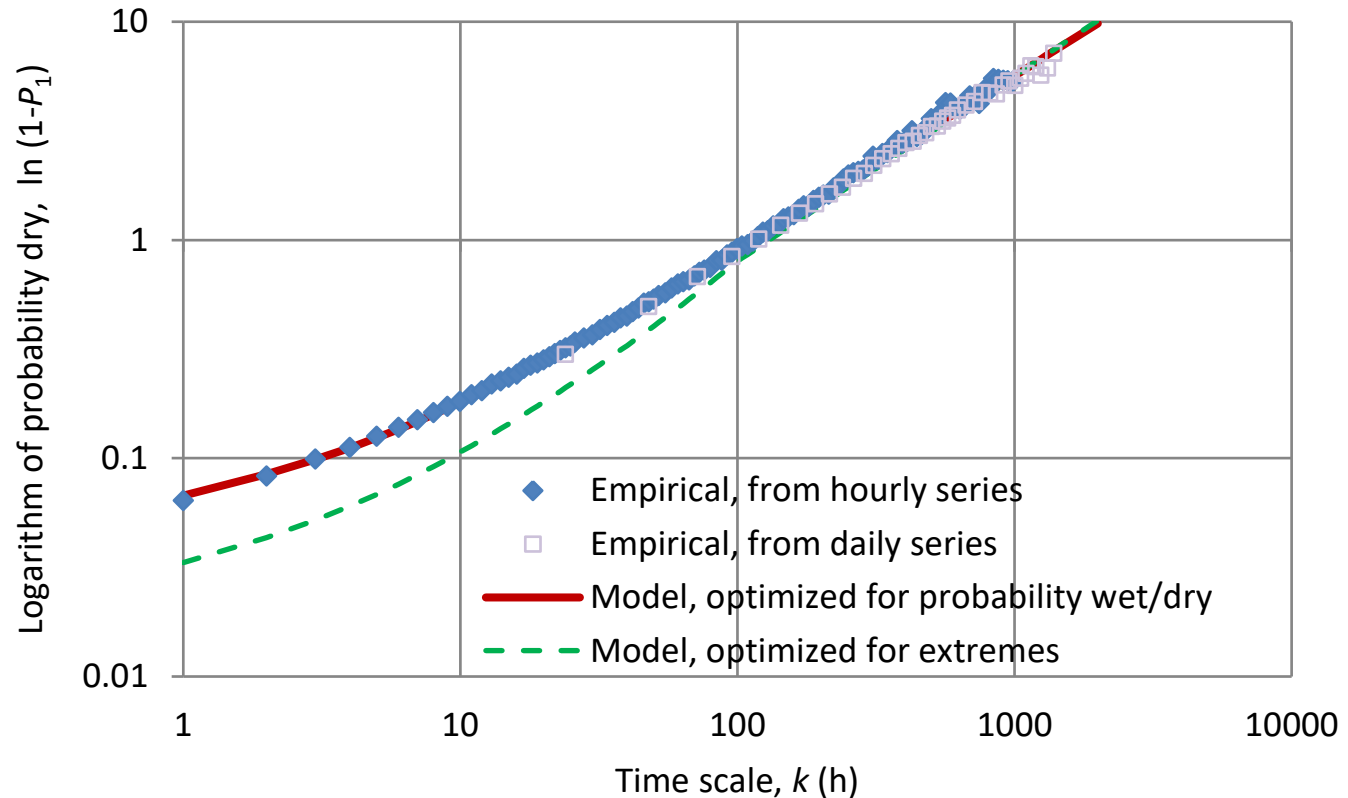
where k^* is the transition time scale from Pareto to PBF distribution, for which $P_0^{(k^*)} > 0$ and $\zeta(k^*) = 1$ (for continuity in the transition point), and θ is a parameter ($0 \leq \theta \leq 1$). This equation has been derived in

Koutsoyiannis (2006) based on maximum entropy considerations.

In the Pareto case, since $\zeta(k) = 1$, the probability wet is fully determined from the other parameters:

$$P_1^{(k)} = \frac{1 - \xi}{1/2 - \xi} \frac{\mu^2}{\gamma(k) + \mu^2}$$

Fitting of the ombrian model to the empirical estimates of probability wet (P_1) or dry ($1 - P_1$).



Mathematical relationships of the ombrian model

Quantity	Small scales, $k \leq k^*$ (Pareto)	Large scales, $k \geq k^*$ (PBF) ¹
$E[\underline{x}^{(k)}]$	μ	
$\gamma(k)$	$\lambda_1(1 + (k/\alpha)^{2M})^{\frac{H-1}{M}}$ or $\lambda_1 \left(1 + \frac{k}{\alpha}\right)^{2H-2} + \lambda_2 \left(1 - \left(1 + \frac{\alpha}{k}\right)^{2H-2}\right)$	
$P_1^{(k)}$	$\frac{1 - \xi}{1/2 - \xi} \frac{\mu^2}{\gamma(k) + \mu^2}$	$1 - \left(1 - P_1^{(k^*)}\right)^{(k/k^*)^\theta}$
$\frac{1}{\zeta(k)}$	1	$\sqrt{(1 - 2\xi) \left(P_1^{(k)} \frac{\gamma(k) + \mu^2}{\mu^2} - 1\right)}$
$\frac{1}{\lambda(k)}$	$\frac{\mu}{(1/2 - \xi)(\gamma(k) + \mu^2)}$	$\left(1 + \frac{1}{(1 - \xi)(\zeta(k))^2} - \frac{1}{(\zeta(k))^{\sqrt{2}}}\right) \frac{P_1^{(k)}}{\mu}$
x for $\xi > 0$	$\lambda(k) \frac{\left(P_1^{(k)} T^{(k)}/k\right)^\xi - 1}{\xi}$	$\lambda(k) \left(\frac{\left(P_1^{(k)} T^{(k)}/k\right)^\xi - 1}{\xi}\right)^{\frac{1}{\zeta(k)}}$
x for $\xi = 0$	$x = \lambda(k) \ln \left(P_1^{(k)} T^{(k)}/k\right)$	$x = \lambda(k) \left(\ln \left(P_1^{(k)} T^{(k)}/k\right)\right)^{\frac{1}{\zeta(k)}}$

The ombrian curves per se are given in the last two rows. The transition time scale k^* has a default value of ~ 100 h.

Parameters of the ombrian model

Parameter	Meaning of parameter	Related tool
μ	Mean intensity	Mean, μ
λ (or λ_1, λ_2)	Variance scale parameters ¹	Climacogram, $\gamma(k)$
α	Time scale parameter	Climacogram, $\gamma(k)$
M	Fractal (smoothness) parameter ²	Climacogram, $\gamma(k)$
H	Hurst parameter	Climacogram, $\gamma(k)$
ξ	Tail index	Probability distribution, $F(x)$
θ	Exponent of the expression of probability dry	Probability wet, $P_1^{(k)}$

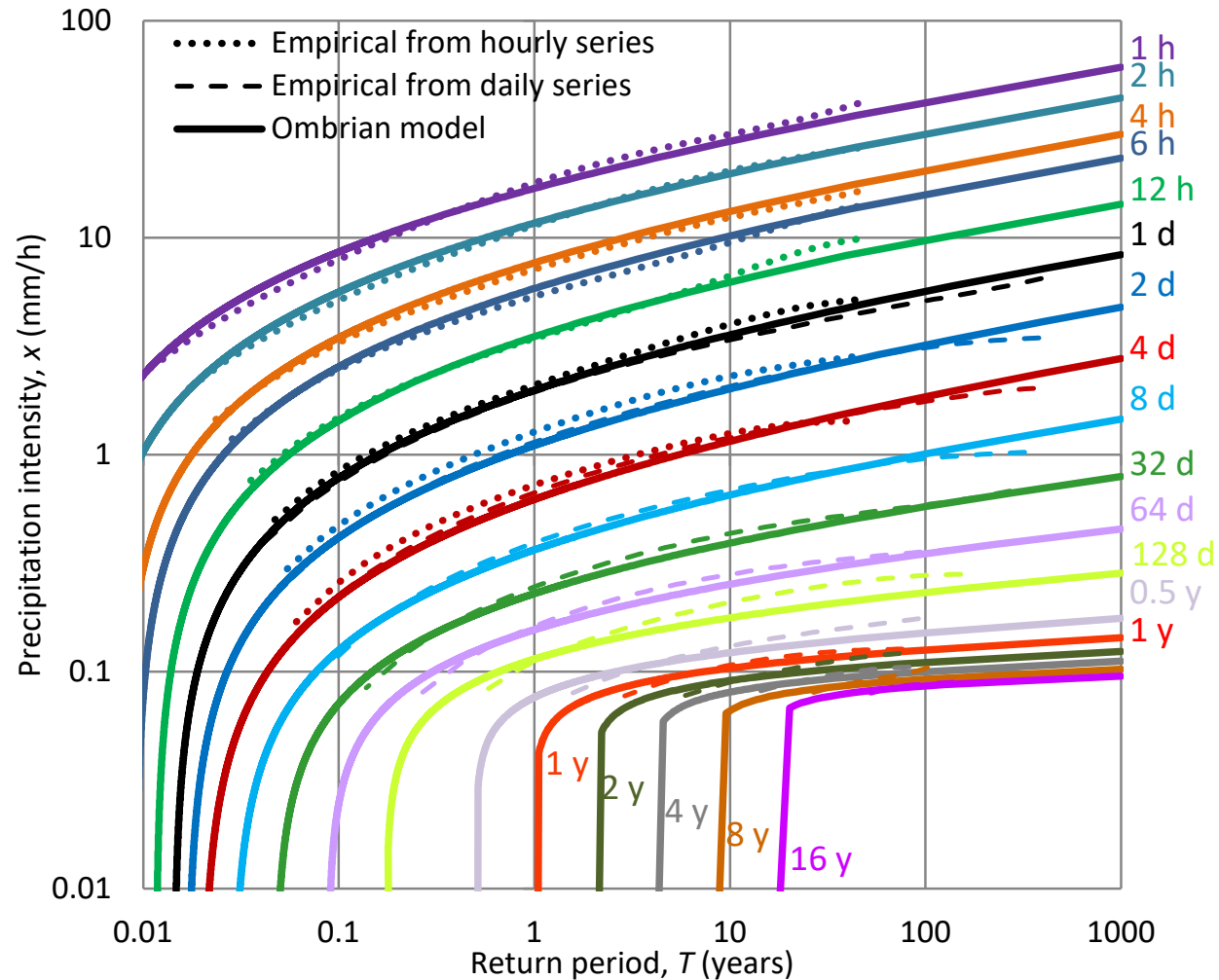
- ¹ One or two parameters for the two cases depending on the choice of the climacogram expression.
- ² The fractal (roughness/smoothness) parameter M is an independent parameter if we have chosen a climacogram expression with one λ ; otherwise it is assumed $M = 1 - H$.
- ³ The transition time scale k^* but this is not regarded a parameter but a modelling choice.

With these seven parameters, the ombrian model achieves:

- (a) mathematical and physical consistency;
- (b) coverage of all time scales (from zero to infinity);
- (c) good representation on the very fine time scales, through the fractal parameter M ;
- (d) good representation on very large time scales, through the Hurst parameter H and the preserved mean μ whose effect becomes important as time scale increases;
- (e) simultaneous treatment and preservation of the climacogram; and
- (f) simultaneous treatment and preservation of the probability dry/wet.

Ombrian curves for Bologna: Comparison of model to K-moment estimates of return period

Ombrian curves as resulted from the ombrian model for Bologna for time scales spanning 5 orders of magnitude (1 h to 16 years = 140 256 h). The empirical points are estimated from K-moments. The effect of persistence was taken into account; the model was plotted with bias-adapted variance in order to be comparable with empirical plots.

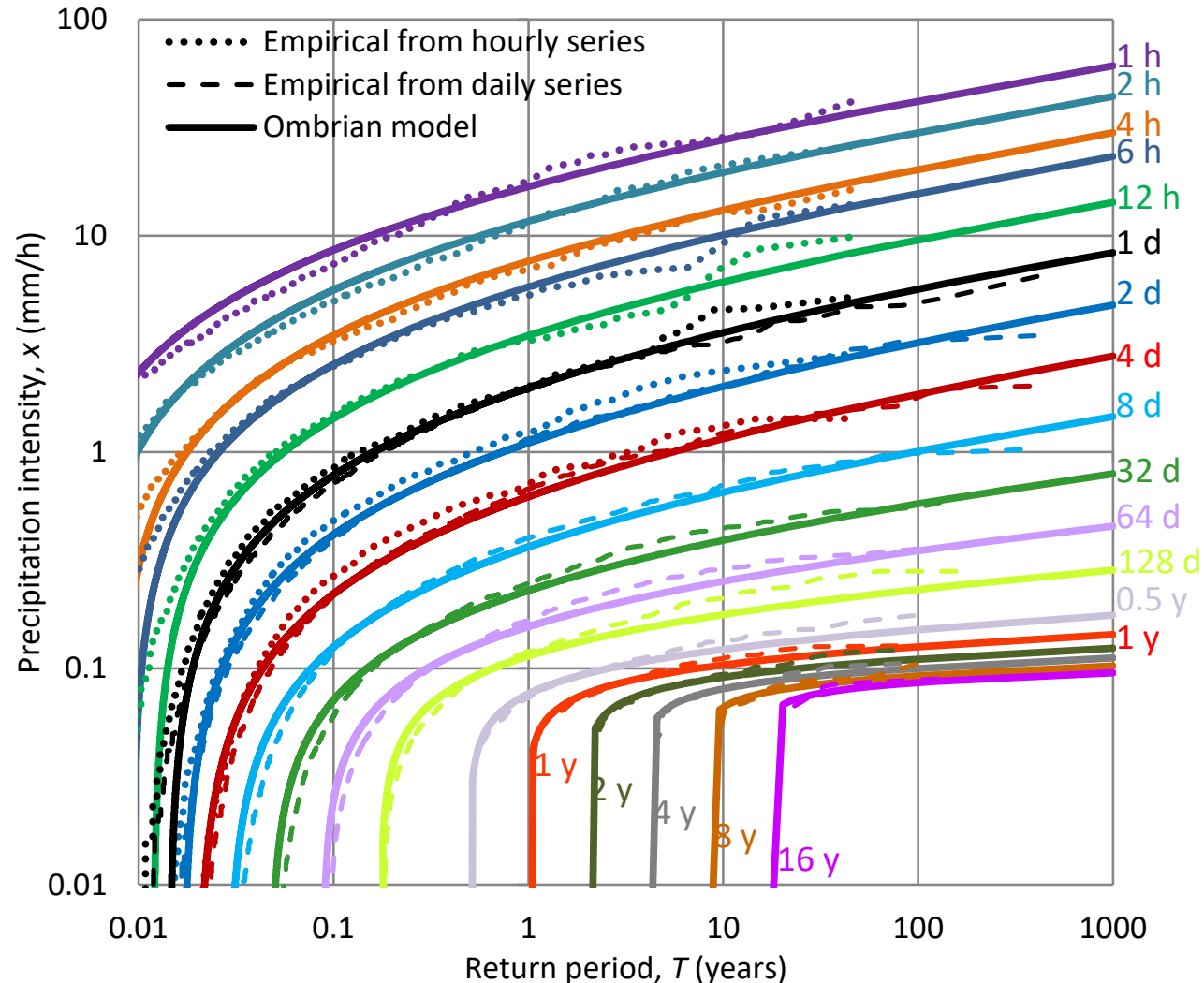


Parameter values	
μ	0.0773 mm/h
λ_1	0.00103 mm ² /h ²
λ_2	1.978 mm ² /h ²
α	9.704 mm
H	0.95
ξ	0.120
θ	0.849

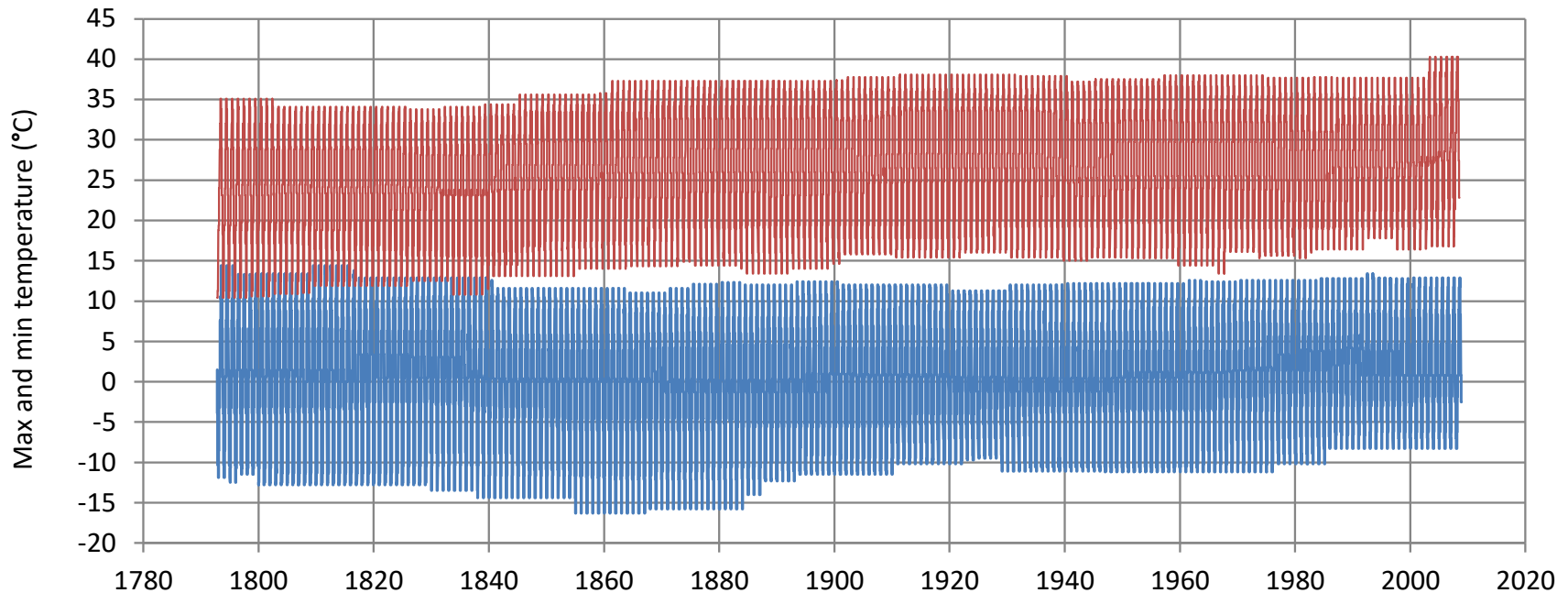
Ombrian curves for Bologna: Comparison of model to order-statistics estimates of return period

Ombrian curves as resulted from the ombrian model for Bologna for time scales spanning 5 orders of magnitude (1 h to 16 years = 140256 h). The empirical points are estimated from order statistics. The effect of persistence was taken into account; the model was plotted with bias-adapted variance in order to be comparable with empirical plots.

Parameter values as in previous page.



Temperature extremes in Milan: A diagnostic analysis of the evolution of climatic extremes in cyclostationary setting



In monthly setting, using a window of 30 years, the plot shows the second highest value out of $\approx 30 \times 30 = 900$ values for the maximum temperature and the second lowest value for minimum ones. The second highest value is a QAD estimate of a K-moment for some order p (see next page). There exist upward and downward fluctuations; the upward ones prevail, particularly in the low extremes.

The climatic range, measured as the difference of the high and low extremes, was 47 °C in 1800, increased to 53 °C in 1860 (worst), decreased to 45 °C in 2000 (best), and increased to 48 °C in 2008.

Assessment of return periods of each of the two extremes

Assuming normal distribution with $\Lambda_\infty = 1.781$, $\Lambda_1 = 2$, the return period of the second highest value among 900 monthly values of 30 years is:

$$\frac{T_{(899:900)}}{(1/30)} = \frac{\Lambda_\infty(900-1)+\Lambda_1}{\Lambda_\infty(900-899)+1} = 576 \Rightarrow T = 19.2 \text{ years}$$

This corresponds to K-moment order:

$$p = \frac{n-(\Lambda_1-\Lambda_\infty)(n-i)}{\Lambda_\infty(n-i)+1} = 323.5$$

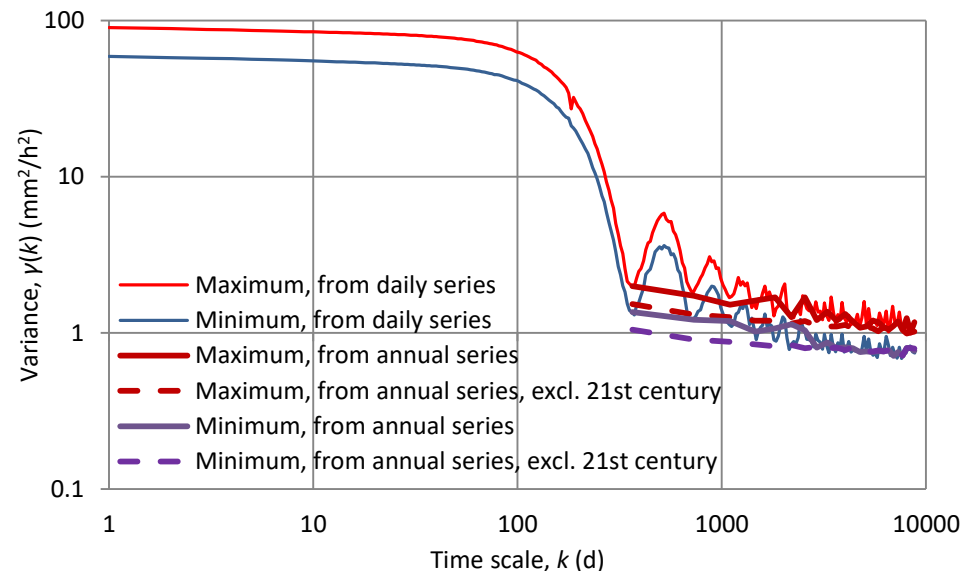
However, both time series suggest strong Hurst-Kolmogorov behaviour, with Hurst parameter $H = 0.93$ (even excluding the 21st century data). For large n the equation on p. 25 can be written as:

$$\theta^{\text{HK}}(n, H) \approx -\frac{1}{2n^{2-2H}} = -\frac{1}{2n'} = -\frac{1}{2} \frac{\gamma_n}{\gamma_1}$$

where n' is the effective sample size; for the Milano daily temperature and $n = 900$, $n' \approx 90/1 = 90$ and $\theta = -0.01$.

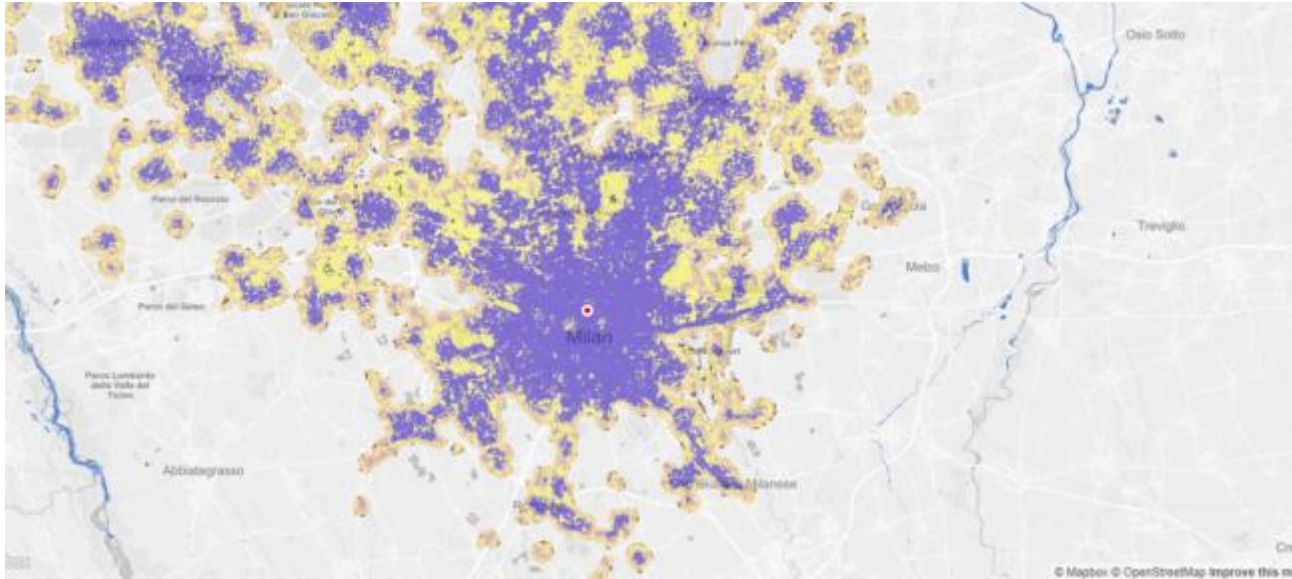
In turn, this results in $p' \approx 2\theta + (1 - 2\theta)p^{((1+\theta)^2)} = 546$ and $T' = 18.2$ years.

This is a rough approximation as the climacograms are of HK type only asymptotically (for large k); stochastic simulation is required for a better approximation.



Climacograms of maximum and minimum daily temperature in Milano.

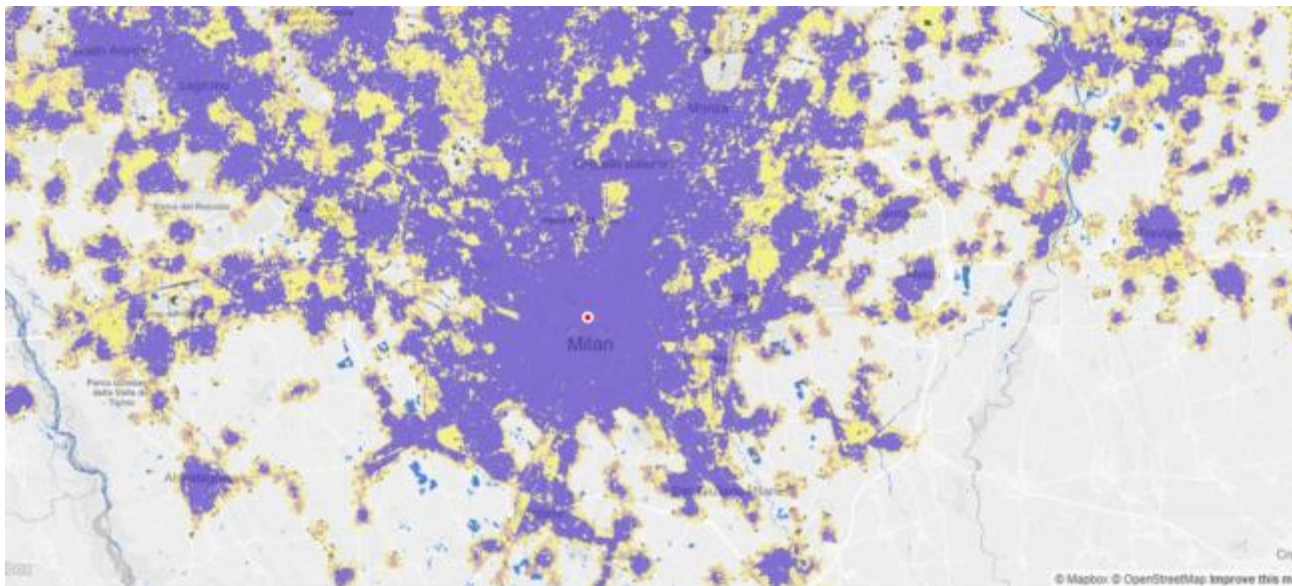
What is the culprit of temperature increase in Milan?



Milan 1988:

Population 3 506 838

Urban extent 88 417 ha



Milan 2013:

Population: 6 402 051

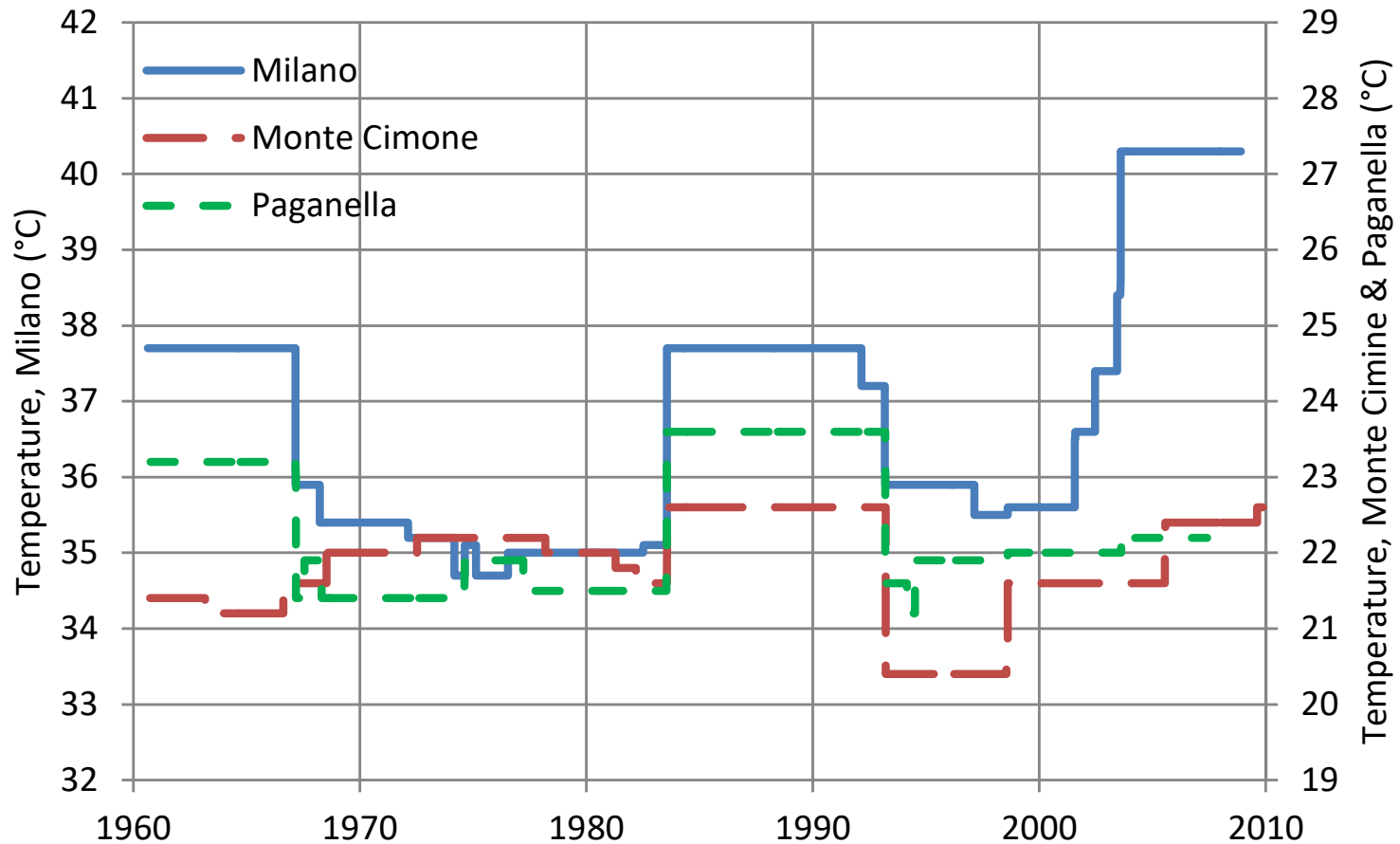
Urban extent 277 177 ha

Graphs: Glynis (2019)

Data: Atlas of Urban Expansion

Comparison with nearby non-urbanized areas

Second highest daily temperature maximum in sliding windows of size 30 years. Note that both Monte Cimone and Paganella stations are in elevations about 2000 m higher than Milan, which causes a temperature difference of $6.5\text{ }^{\circ}\text{C}/\text{km} \times 2\text{ km} = 13\text{ }^{\circ}\text{C}$.



It appears that urbanization is the principal factor causing temperature increase non-urban stations have not been affected.

If we assume that Milan is affected by global warming, can we use climate model results for future prediction?

Tyralis and Koutsoyiannis (2017) have proposed a method to incorporate one or many deterministic forecasts, such as those of climate models, into an initially independent stochastic model.

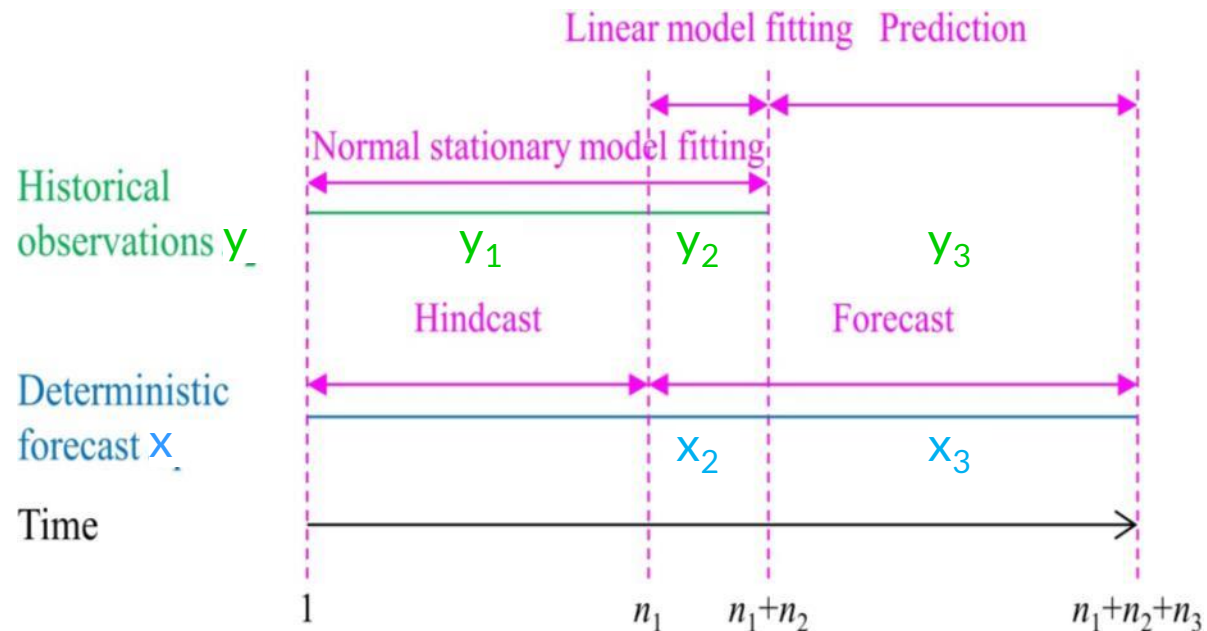
If the deterministic forecasts are good, then the Bayesian framework proposed takes them into account, otherwise they are automatically disregarded.

With reference to the sketch on the right, we simulate the unknown future y_3 conditional on the known past y_1, y_2 and the deterministic model outputs x_2, x_3 by:

$$h(y_3|y_1, y_2, x_2, x_3) \propto f(x_3|y_3) g(y_3|y_1, y_2)$$

where $f(x_3|y_3)$ is the model likelihood (evaluated from x_2 and y_2) and the other functions are conditional densities.

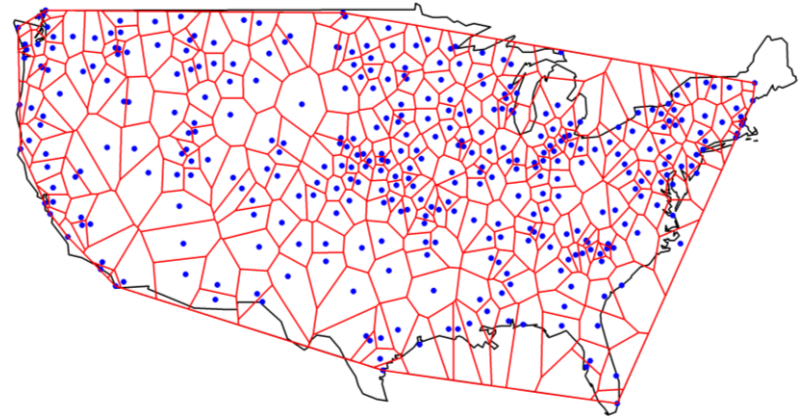
The method was tested on large data sets in the USA (not yet in Italy).



Example of climate model testing in the USA

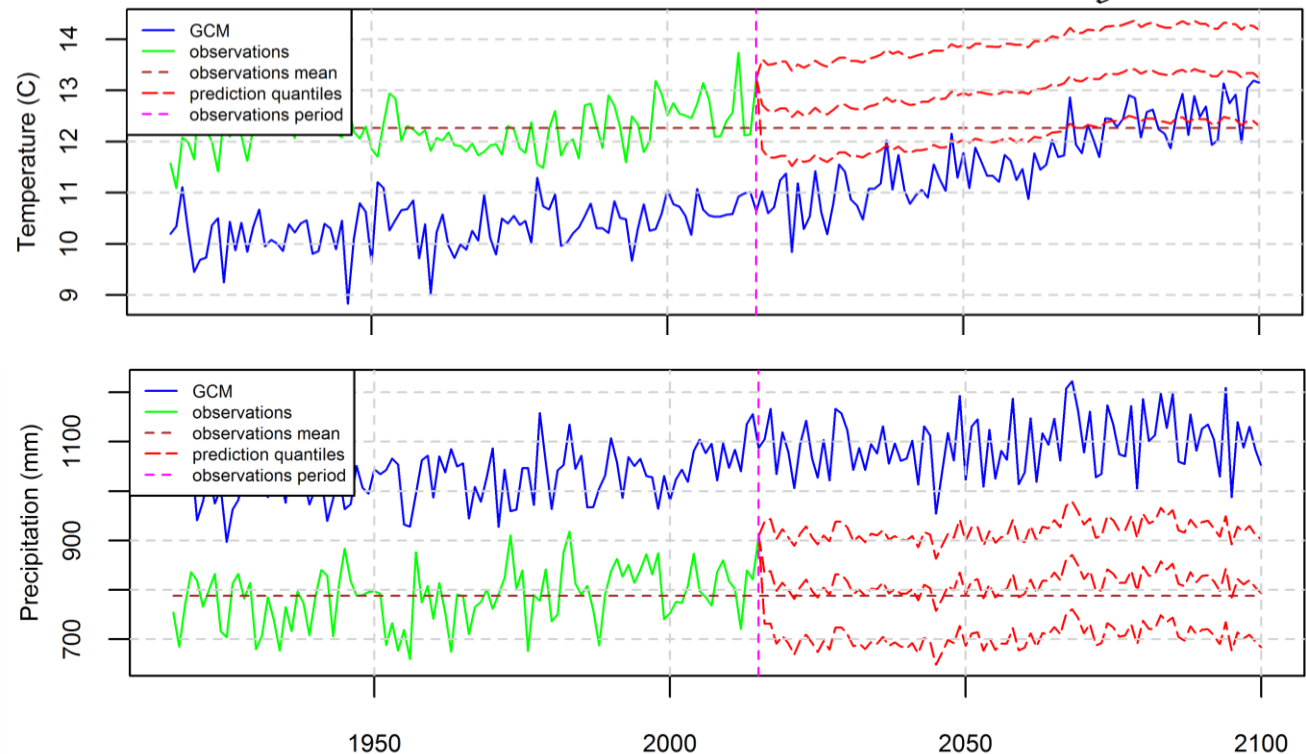
Historical data for temperature and precipitation from 362 and 319 stations, respectively, have been used to estimate the areal averages (historical observations).

Deterministic forecasts were taken from 14 different climate models. The model likelihood was evaluated in the period 2006-15.



The example on temperature (95% prediction intervals) shows a slight increase in annual temperature in the USA if conditioned on the output of MRI-CGCM3 climate model.

The example on precipitation shows indifference despite conditioning on the GISS-E2-H climate model.



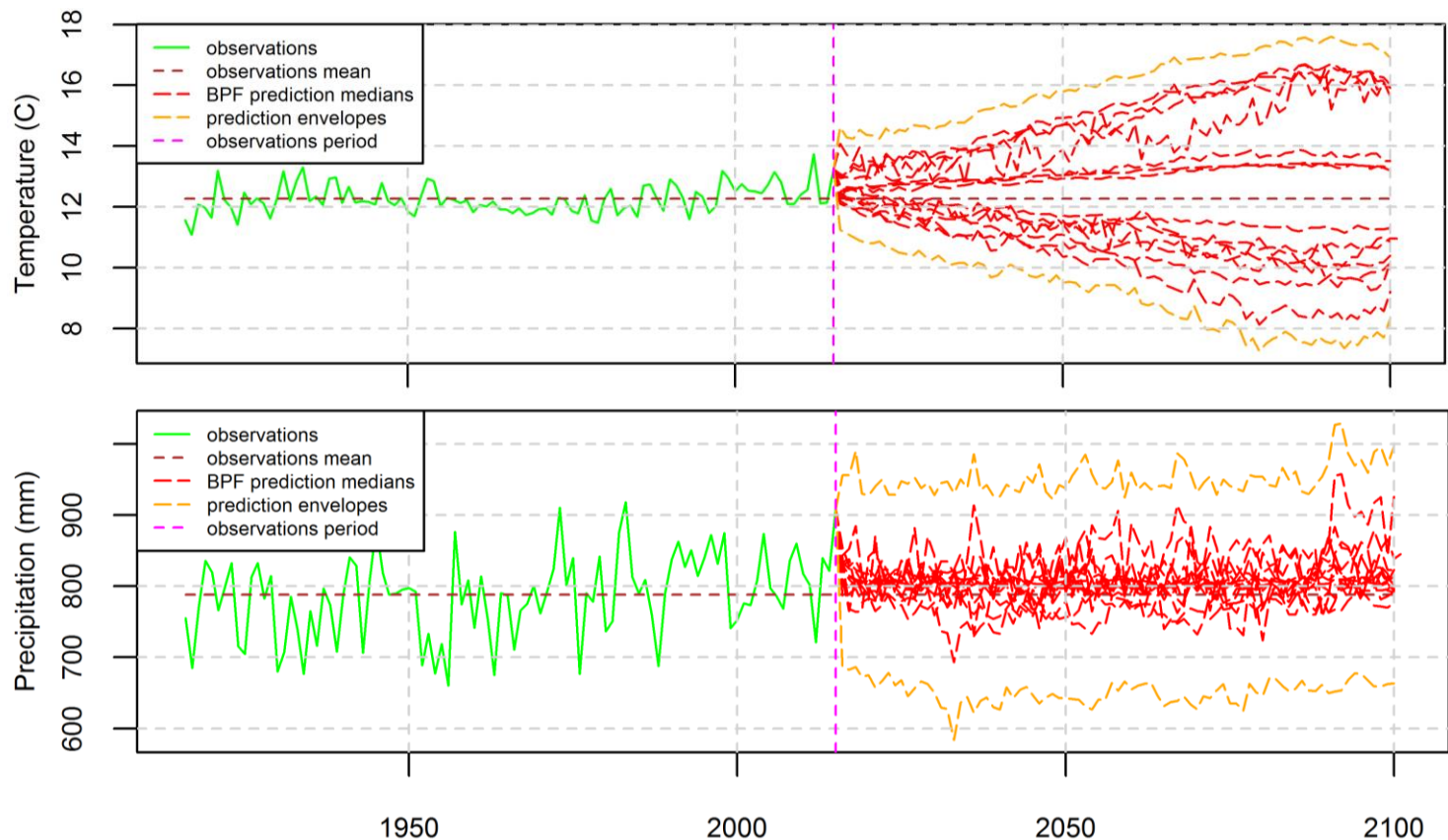
Final multimodel results for temperature and precipitation in the USA

If all models are taken into account, the temperature change up to 2100 could be somewhere in the range -4 to 4 °C. The negative predictions result from the fact that some models have negative correlation with historical data!

Precipitation does not change by conditioning on all models. Only its uncertainty increases slightly (± 50 mm, if compared to that without conditioning on models).

General conclusion:

Climate model predictions (or projections) can hardly justify a reason to be incorporated in studies of real world processes.



Stochastic forecast-oriented estimation

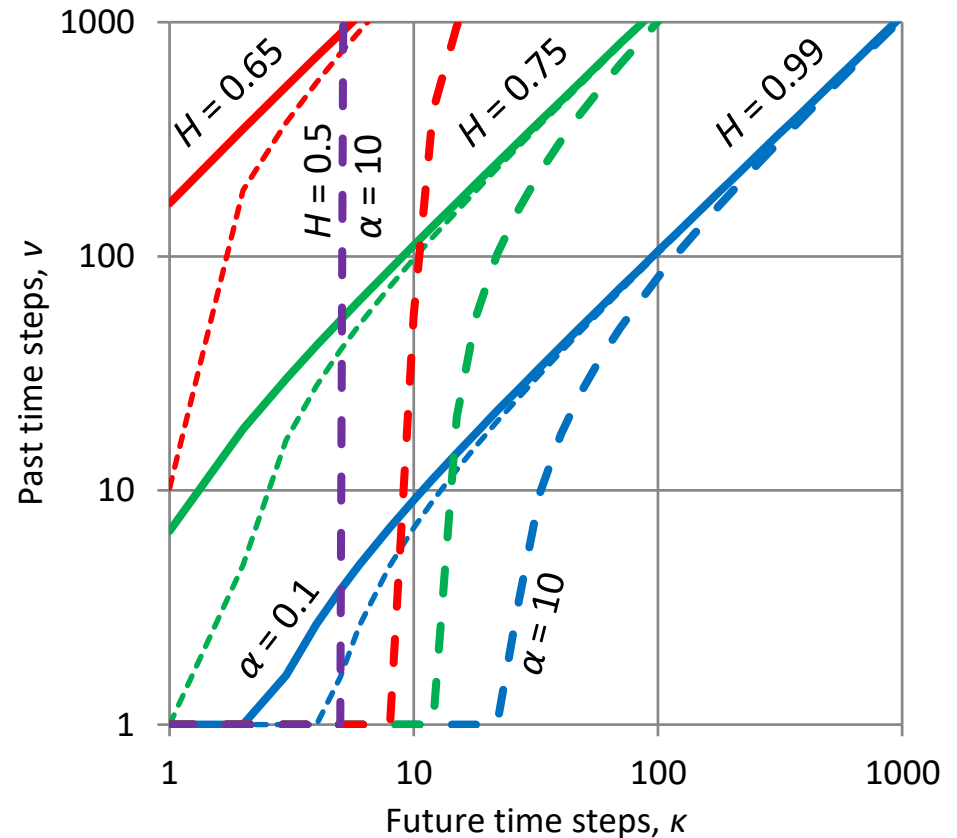
The process mean is a neutral predictor of the future (zero efficiency) but in most cases is better than climate model predictions (negative efficiency).

However, because in real world processes there is dependence in time, a local mean (of a few recent values) can be a better predictor than the global (or the true) mean, as well as than trend models (Iliopoulou and Koutsoyiannis, 2019).

In particular, for the FHK-C model (with climacogram $\gamma(\kappa) = \lambda(1 + \kappa/\alpha)^{2H-2}$), if we wish to predict a future time window of length κ , then the optimal value ν of the number of past terms, forming the local mean, is (Koutsoyiannis, 2020):

$$\nu \approx \max\left(1, \frac{\kappa - 2.3(\alpha + 1)H^2 - 1}{(\max(0, 2.5H - 1.5))^{2.5}}\right)$$

It can be seen in the graph on the right that there are cases (for large H and α) that the optimal ν can be as small as 1; this means that the present value of the process, rather than the mean of the past, should be used as the predictor of the future (even though the process is stationary).



Conclusions

- Trend following may mean taking steps back. Therefore: **better classic than trendy** (cf. Iliopoulou and Koutsoyiannis, 2019).
- In a non-trendy (meaning **stationary and ergodic**) framework, the newly introduced knowable moments (K-moments) are powerful tools that unify other statistical moments (classical, L-, probability weighted) and order statistics, offering several advantages.
- In particular, they offer a sound basis for distribution fitting with emphasis on extremes.
- For **independent** identically distributed variables, K-moments offer **unbiased**, reliable and workable estimators for low and high orders p , up **to order equal to the sample size n** .
- **Time dependence influences the estimates**, yet K-moments offer a basis to assess that influence and properly adapt the estimates.
- Rainfall extremes can be effectively modelled by a rather simple ombrian model, which, in addition to modelling extremes, provides a good representation the climacogram of the rainfall process and its intermittence.
- For temperature extremes further research is required.

References

- Bacchi, B., Becciu, G. and Kottegodu, N.T., 1994. Bivariate exponential model applied to intensities and durations of extreme rainfall. *Journal of Hydrology*, 155(1-2), 225-236.
- Bacchi, B., Brath, A. and Kottegodu, N.T., 1992. Analysis of the relationships between flood peaks and flood volumes based on crossing properties of river flow processes. *Water Resources Research*, 28(10), 2773-2782.
- Bacchi, B. and Ranzi, R., 1996. On the derivation of the areal reduction factor of storms. *Atmospheric Research*, 42(1-4), 123-135.
- Balistracchi, M. and Bacchi, B., 2011. Modelling the statistical dependence of rainfall event variables through copula functions. *Hydrology and Earth System Sciences*, 15(6), 1959-1977.
- Donat, M.G., Lowry, A.L., Alexander, L.V., O’Gorman, P.A., and Maher, N., 2016. More extreme precipitation in the world’s dry and wet regions. *Nature Climate Change*, 6, doi: 10.1038/NCLIMATE2941.
- Glynis, K., 2019. Stochastic investigation of the behavior of land surface air temperature on global scale. Diploma thesis, 159 pp., Athens, www.itia.ntua.gr/2008/.
- Iliopoulou, T., and Koutsoyiannis, D., 2019. Projecting the future of rainfall extremes: better classic than trendy (in review).
- Koutsoyiannis, D. 2006. An entropic-stochastic representation of rainfall intermittency: The origin of clustering and persistence. *Water Resources Research*, 42(1), W01401, doi:10.1029/2005WR004175.
- Koutsoyiannis, D., 2013. Hydrology and Change. *Hydrological Sciences Journal*, 58 (6), 1177–1197, doi: 10.1080/02626667.2013.804626.
- Koutsoyiannis, D., 2019. Knowable moments for high-order stochastic characterization and modelling of hydrological processes. *Hydrological Sciences Journal*, 64(1), 19–33, doi:10.1080/02626667.2018.1556794.
- Koutsoyiannis, D. (2020), *Stochastics of Hydroclimatic Extremes – A Cool Look at Risk* (in preparation).
- Koutsoyiannis, D., and Montanari, A., 2015. Negligent killing of scientific concepts: the stationarity case. *Hydrological Sciences Journal*, 60(7-8), 1174–1183, doi: 10.1080/02626667.2014.959959.
- Lombardo, F., Volpi, E., Koutsoyiannis, D., and Papalexioiu, S.M., 2014. Just two moments! A cautionary note against use of high-order moments in multifractal models in hydrology. *Hydrology and Earth System Sciences*, 18, 243–255, doi:10.5194/hess-18-243-2014.
- Lombardo, F., Napolitano, F., Russo, F., and D. Koutsoyiannis, D., 2019. On the exact distribution of correlated extremes in hydrology. *Water Resources Research*, doi:10.1029/2019WR025547.
- Milly, P.C.D., Betancourt, J. Falkenmark, M. Hirsch, R.M. Kundzewicz, Z.W. Lettenmaier, D.P. and Stouffer, R.J., 2008. Stationarity Is Dead: Whither Water Management?. *Science*, 319, 573-574.
- Montanari, A., and Koutsoyiannis, D., 2014. Modeling and mitigating natural hazards: Stationarity is immortal!. *Water Resources Research*, 50 (12), 9748–9756, doi: 10.1002/2014WR016092.
- Tsaknias, D., Bouziotas, D., and Koutsoyiannis, D., 2016. Statistical comparison of observed temperature and rainfall extremes with climate model outputs in the Mediterranean region, *ResearchGate*, doi: 10.13140/RG.2.2.11993.93281.
- Tyralis, H., and Koutsoyiannis, D., 2017. On the prediction of persistent processes using the output of deterministic models. *Hydrological Sciences Journal*, 62 (13), 2083–2102, doi: 10.1080/02626667.2017.1361535.
- Volpi, E., Fiori, A., Grimaldi, S., Lombardo, F., and Koutsoyiannis, D., 2019. Save hydrological observations! Return period estimation without data decimation. *Journal of Hydrology*, doi:10.1016/j.jhydrol.2019.02.017.

Data sources

GHCN Version 3 data: retrieved on 2019-02-17 from <https://climexp.knmi.nl/gdcnprcp.cgi?WMO=ITE00100550>

Dext3r data: retrieved on 2019-02-17 from <http://www.smr.arpa.emr.it/dext3r/>

Atlas of Urban Expansion: retrieved on 2019-11-17 from <http://www.atlasofurbanexpansion.org/cities/view/Milan>